

Summary of Key Technologies: Working Group D

Jim Clarke (STFC Daresbury Laboratory), Sara Casalbuoni (European XFEL), Dmitry Bazyl (DESY), Olivier Marcouille (SOLEIL), and Nishimori Nobuyuki (QST)

Key Technologies Working Group D

- 19 presentations across 5 sessions
- Thanks to all the speakers for your excellent, high quality, presentations
- We covered a very broad range of topics...
 - Superconducting RF
 - Normal conducting RF (warm and cold)
 - RF Power sources
 - RF photoinjectors and photocathodes
 - Femtosecond synchronisation
 - Advanced diagnostics for XFELs and Storage Rings
 - Undulators of various types (SC wire, SC bulk, bi-periodic)
 - Machine Learning
 - Vacuum
 - New software tools

Daniel Gonnella (SLAC), ID: 2065 - TU3D1
Developments in SRF Technology for Light
Source Applications

The name of the game is Q_0

2010

EU-XFEL Cavity
Construction

2013

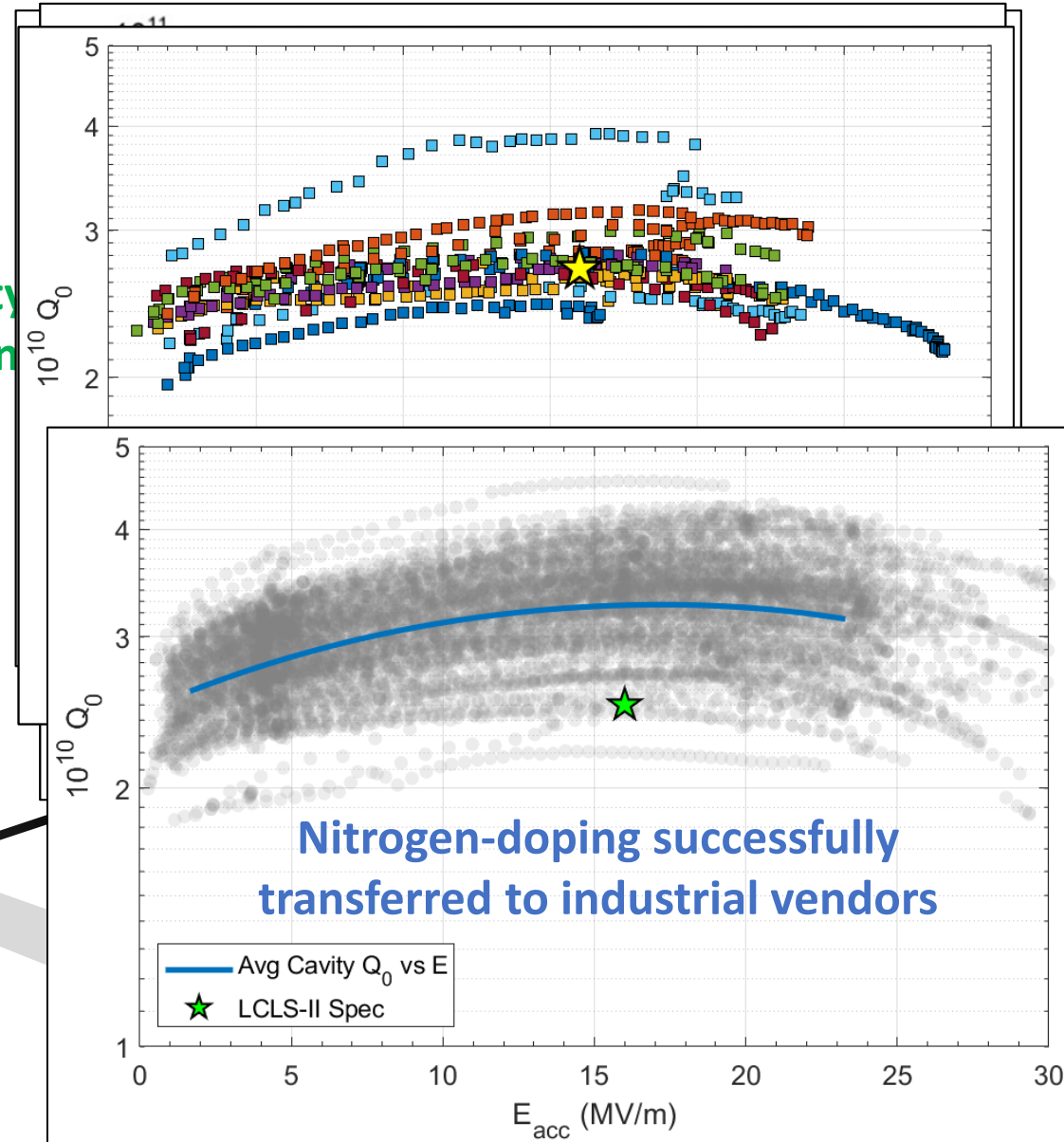
Discovery of N-Doping

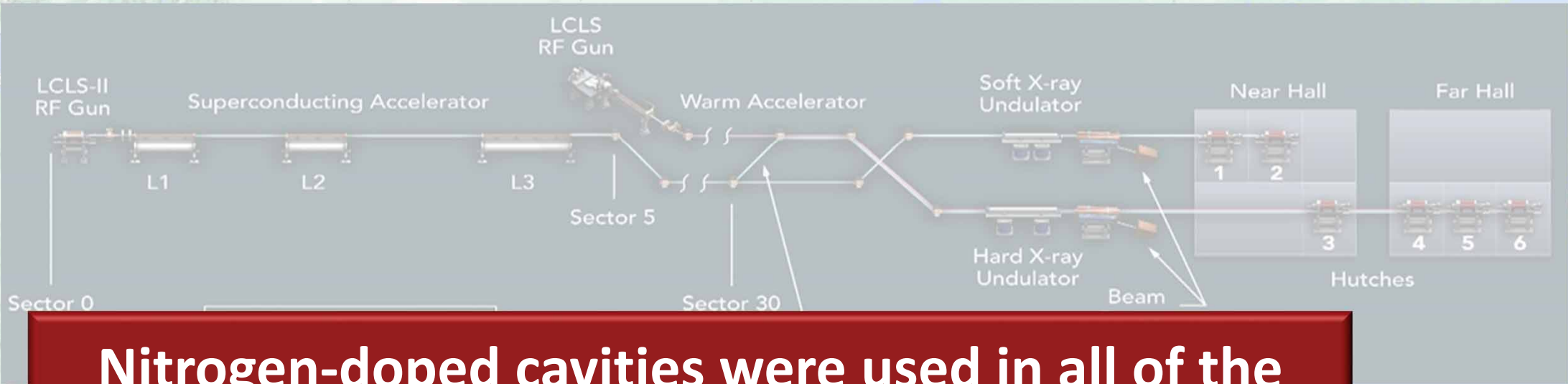
2016

LCLS-II Cavity
Construction

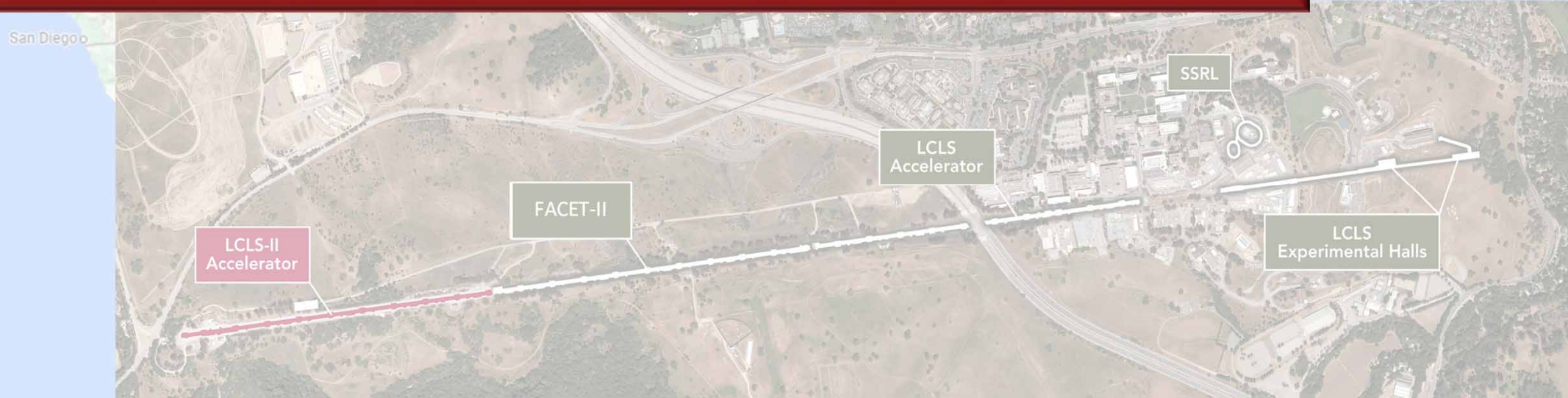
2014-2016

LCLS-II High Q_0 R&D





Nitrogen-doped cavities were used in all of the 1.3 GHz LCLS-II Cryomodules – first use of the new technology in an installed accelerator

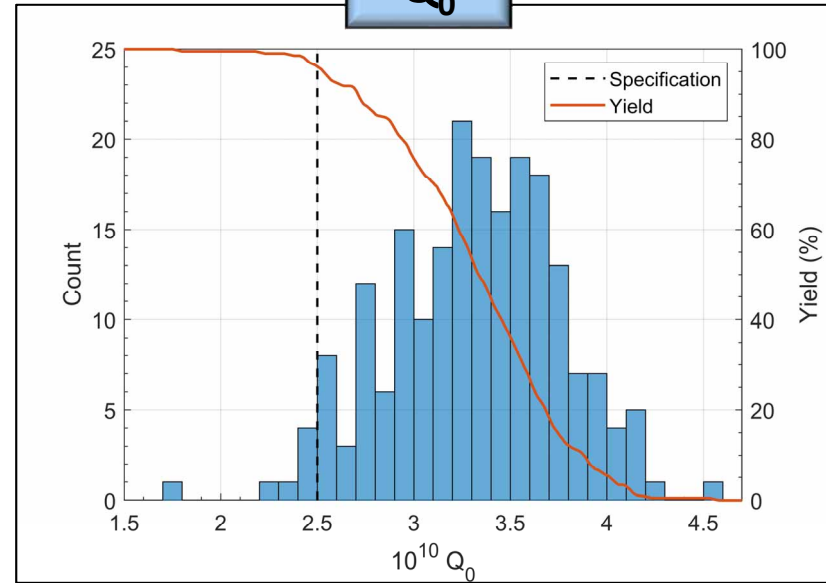
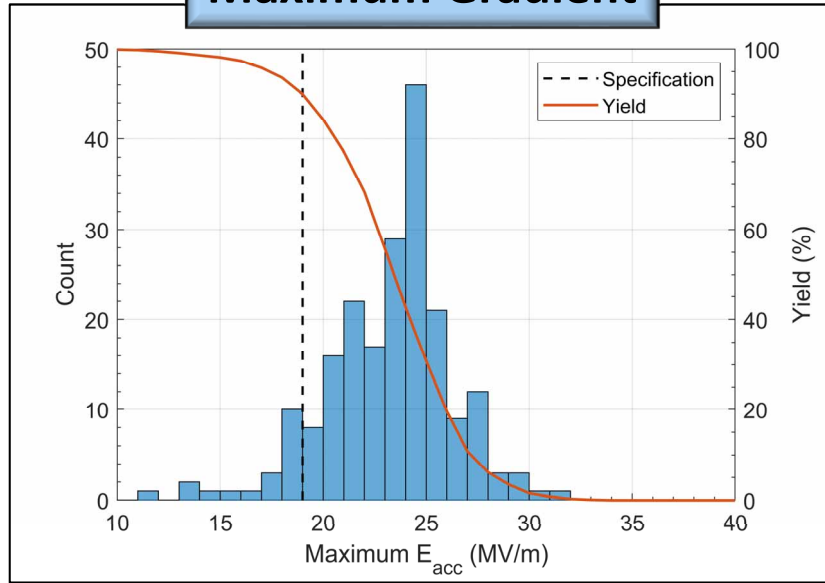


LCLS-II-HE: Cavity Performance Improvements

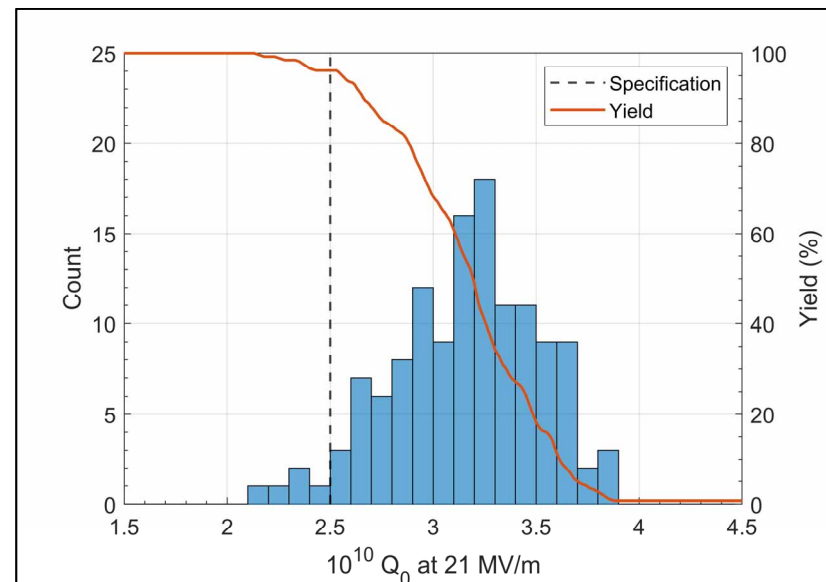
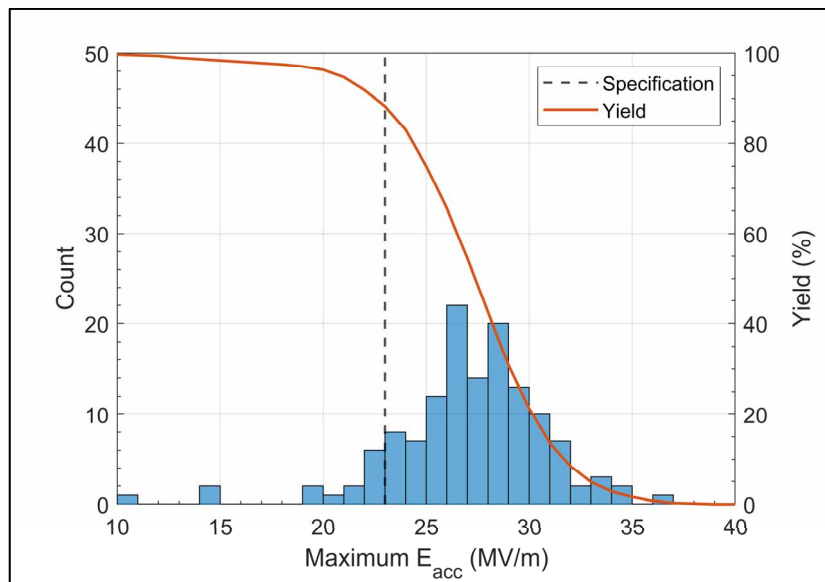
Maximum Gradient

Q_0

LCLS-II



LCLS-II-HE



- Average maximum gradient **increased by ~4 MV/m**
- Average Q_0 unchanged

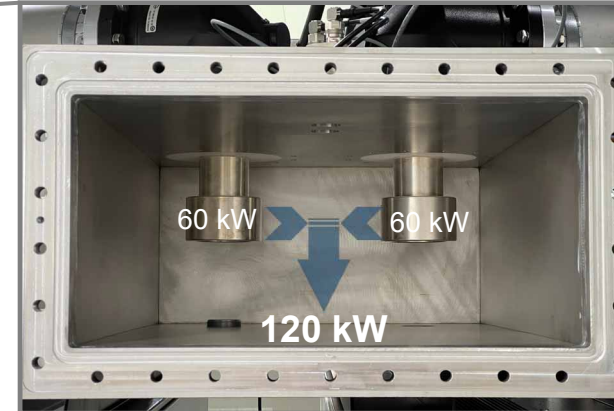
**20.8MV/m for HE
Compared to
16MV/m for LCLS-II**

Marcus Lau (TRUMPF GmbH) ID: 2313 -
TU3D2 Highly Reliable RF Power Sources for
Improvement of the Accelerator Availability

TruAccelerate

120kW Solid State System architecture at 500MHz for Synchrotron Light Sources

2:1 Combining step from coaxial to waveguide



HMI displaying the amplifier status down to the pallet level



MTBF and AFR values

for the complete Rack and individual PA Units, DCUs and PDUs

$$MTBF_{Rack} = 166,750 \text{ [h]} \quad AFR_{Rack} = 5.12\%$$

$$MTBF_{PA \text{ Unit}} = 952,857 \text{ [h]} \quad AFR_{PA \text{ Unit}} = 0.92\%$$

$$MTBF_{DCU} = 833,750 \text{ [h]} \quad AFR_{DCU} = 1.05\%$$

$$MTBF_{PDU} = 1,667,500 \text{ [h]} \quad AFR_{PDU} = 0.52\%$$



$$MTBF_{Rack} = 555,833 \text{ [h]} \quad AFR_{Rack} = 1.56\%$$

$$MTBF_{PA \text{ Unit}} = 6,670,000 \text{ [h]}^* \quad AFR_{PA \text{ Unit}} = 0.13\%$$

* We assumed that a PA Unit could fail in any coming time. This value is 0 at the moment for data taken

Emilio Alessandro Nanni (SLAC) ID: 2141 -
TU3D3 Application of Cryo-copper
Accelerating Structures Towards Future
Light Sources

Cryo-Copper: Enabling Efficient High-Gradient Operation

Cryogenic temperature elevates performance in gradient

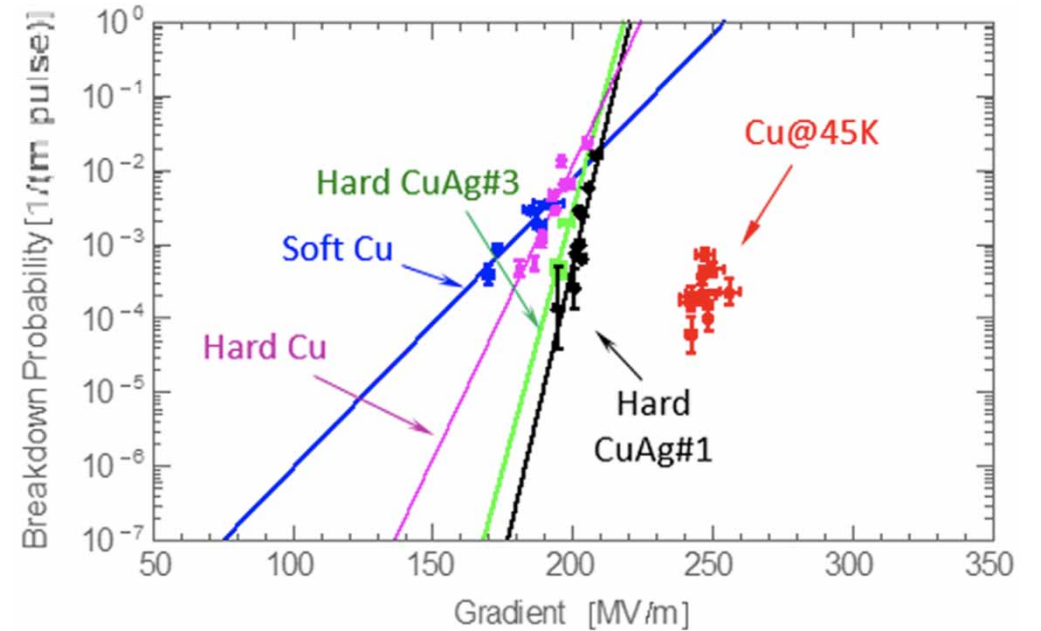
- Increased material strength is key factor
- Increase electrical conductivity reduces pulsed heating in the material

Operation at 77 K with liquid nitrogen is simple and practical

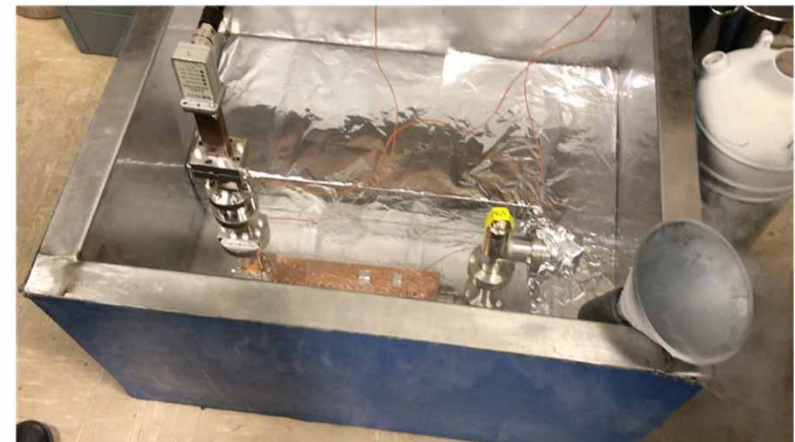
- Large-scale production, large heat capacity, simple handling
- Small impact on electrical efficiency

$$\begin{aligned} \eta_{cp} &= \text{LN Cryoplant} \\ \eta_{cs} &= \text{Cryogenic Structure} \\ \eta_k &= \text{RF Source} \\ \frac{\eta_{cs}}{\eta_k} \eta_{cp} &\approx \frac{2.5}{0.5} [0.15] \approx 0.75 \end{aligned}$$

FLS 2023



Cahill, A. D., et al. *PRAB* 21.10 (2018): 102002.





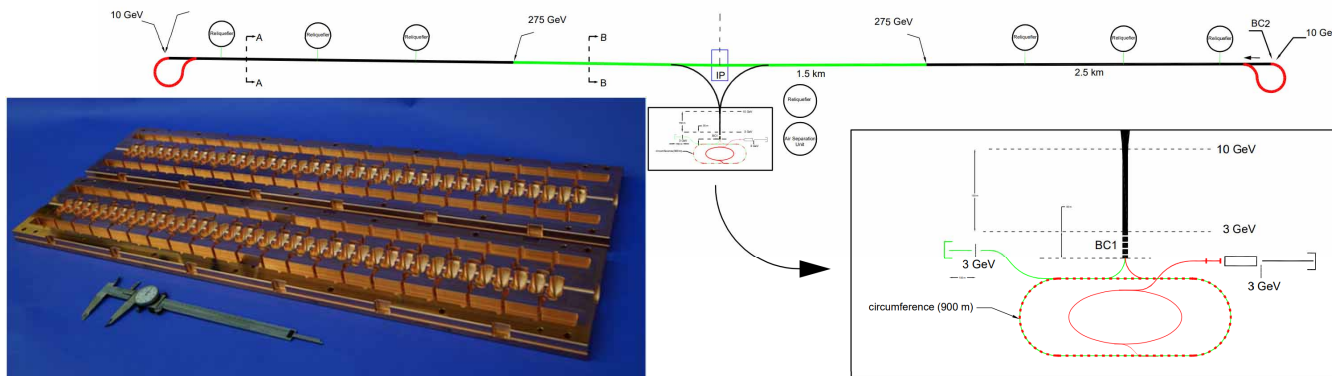
Cool Copper Collider as a Higgs Factory

C³ is based on cryogenic operation and distributed rf coupling

- Dramatically improving efficiency and breakdown rate

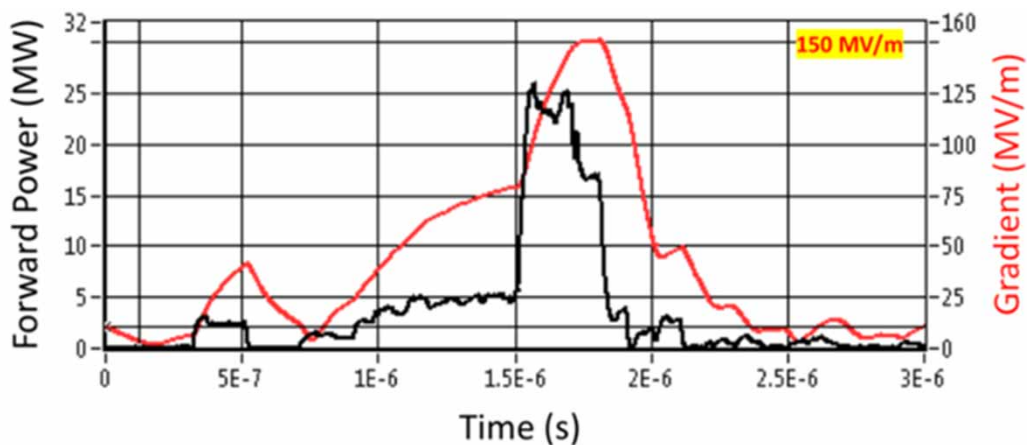
Robust operations at high gradient: 120 MeV/m
Target 250/550 GeV center of mass with 70/120 MeV/m in an 8 km footprint

C³ 250/550 GeV 8 km Site to Scale



C³ Prototype One Meter Structure

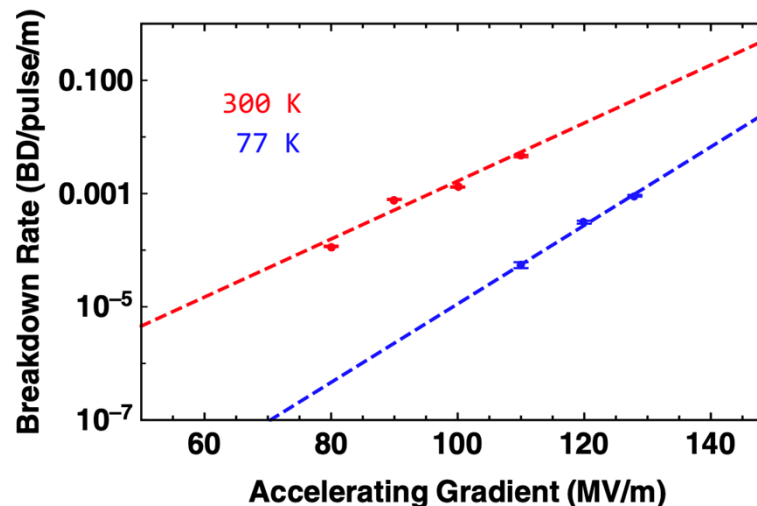
High Gradient Operation at 150 MV/m



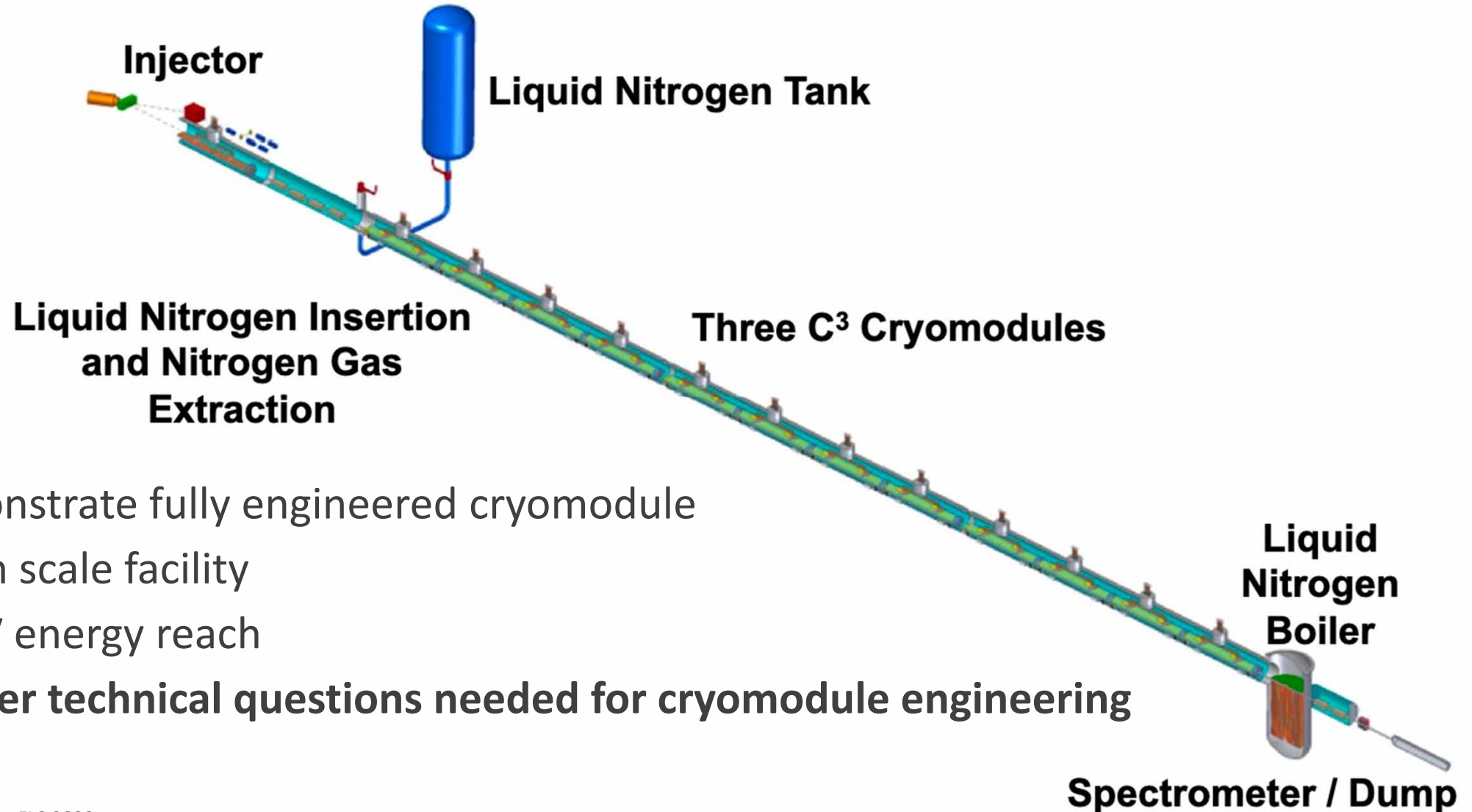
Cryogenic Operation at X-band

PHYS. REV. ACCEL. BEAMS 24, 093201 (2021)

Improvement in Breakdown Rate



The Complete C³ Demonstrator



Demonstrate fully engineered cryomodule

~50 m scale facility

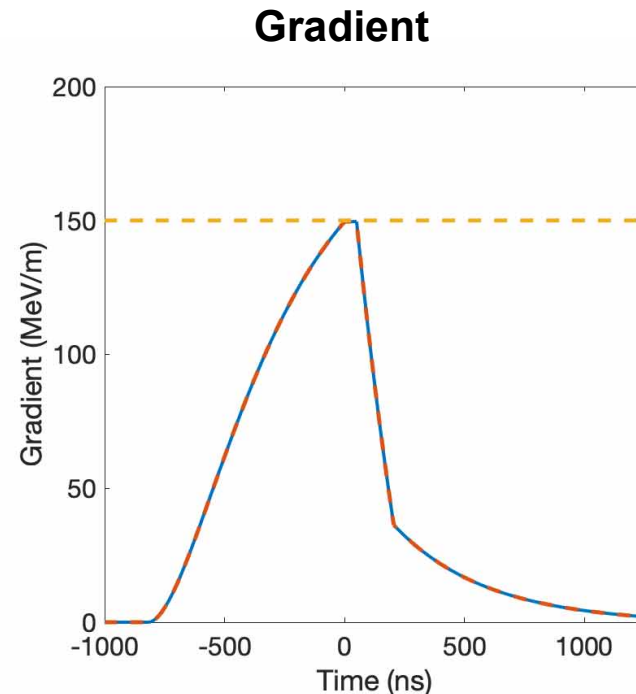
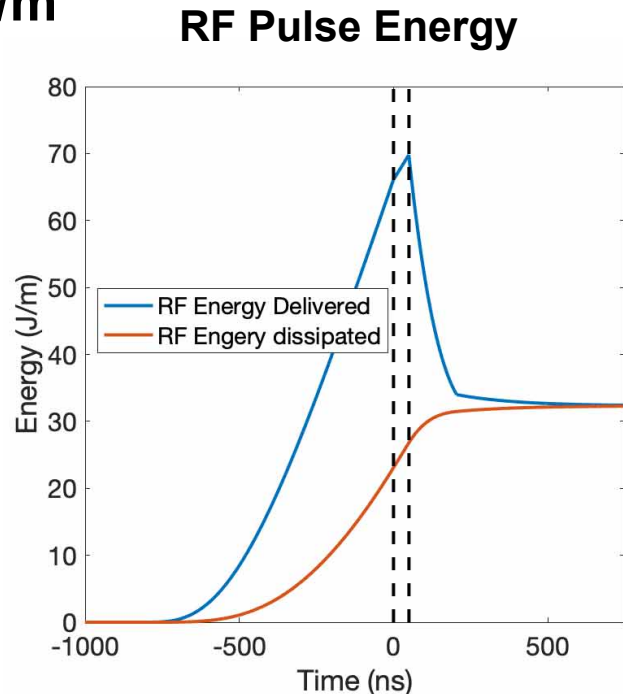
3 GeV energy reach

Answer technical questions needed for cryomodule engineering

High Repetition Rate Operation

- Reduced thermal load at high gradient with cryogenic operation
- Depends strongly on desired gradient and length of flat top
- Assuming 10 micron alignment -> ~15 kW/m thermal load

Example: C-band, No RF Pulse Compression, 140 MW/m, 150 MeV/m, 50 ns Flat Top, 480 Hz, 15 kW/m



Lowest Frequency for Specified Rep. Rate

- 10 kHz Operation – 50 MeV/m – X-band
- 1 kHz Operation – 100 MeV/m – X-band
- 1 kHz Operation – 70 MeV/m – C-band
- 360 Hz Operation – 120 MeV/m – C-band
- 120 Hz Operation – 150 MeV/m – S-band

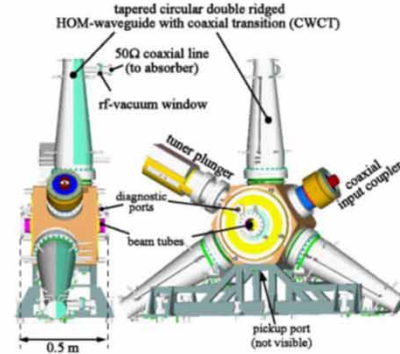
Hiroyasu Ego (KEK) ID: 2223 - TU3D4
Compact HOM-damped RF Cavity for a Next
Generation Light Source

RF cavity with compact HOM-damping structure

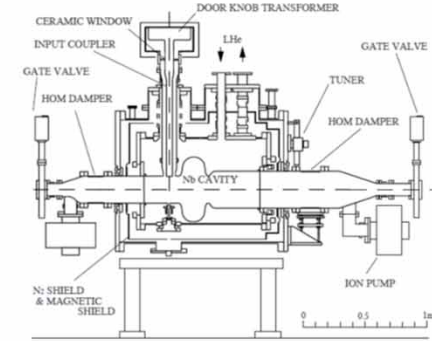
Here →



Existing HOM-damped cavities



E. Wehreter, EPAC08, p.2936



T. Furuya et al., PAC97, p.3087

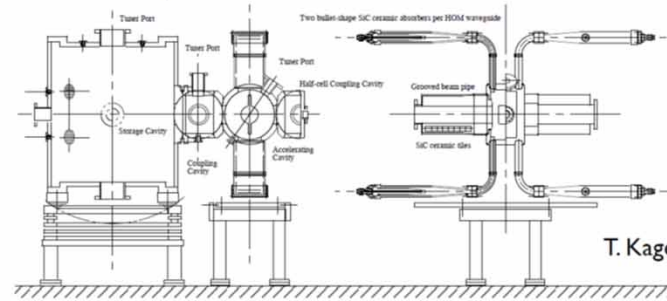


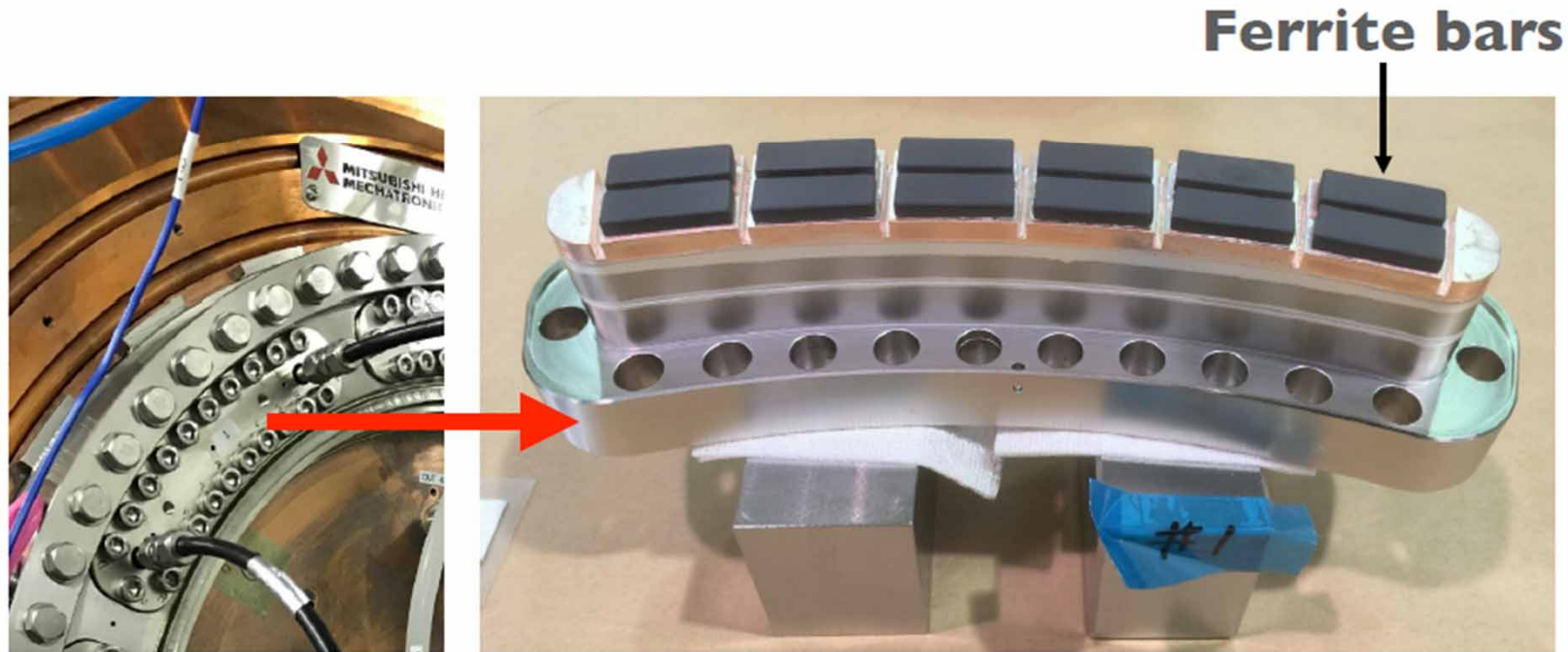
Figure 1: A schematic drawing of ARES96

T. Kageyama et al., PAC97, p.2902

**Massive cavities
with HOM-damping waveguides or/and pipes**

16 HOM dampers directly embedded into the cavity body

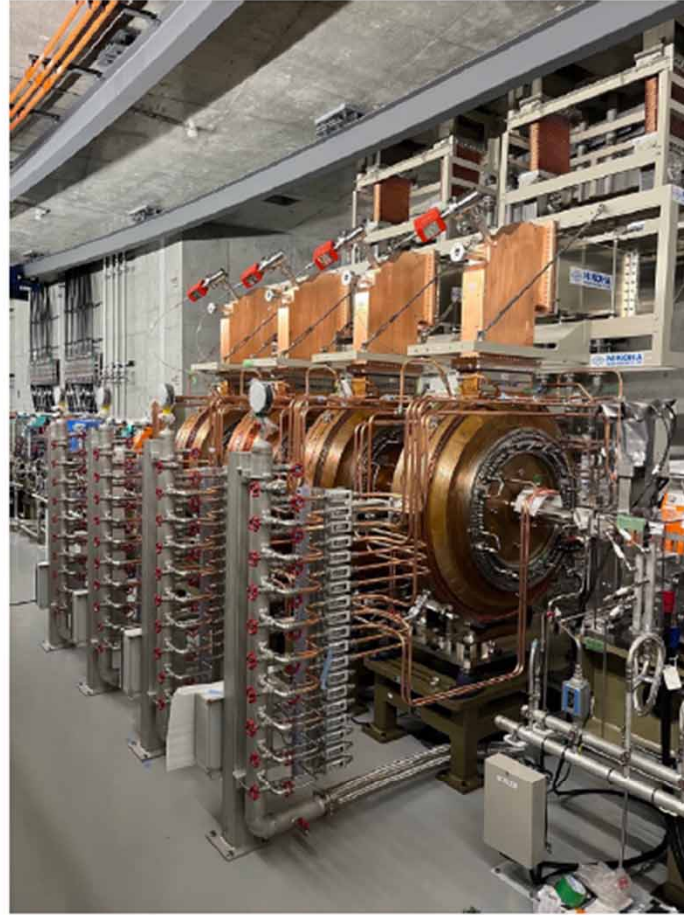
HOM damper



- **Ferrite bars brazed to the curving flange**
- **Water cooling channel provided in flange**
- **No change in cavity size by installing HOM dampers**

Cavities in NanoTerasu

NanoTerasu : 3 GeV Next Generation Light Source in Japan



Four cavities have begun to accelerate a beam

Boris Militsyn (STFC Daresbury) ID: 2482 -
TU3D5 Electron RF Injectors for Next
Generation FELs

Typical requirements to the beams for next generation FELs

Wavelength of a photon with given energy is defined as:

$$\lambda = \frac{hc}{eU}$$

That gives 62 pm at U=20 keV (HXR) and 13.4 nm for U=100 eV (SXR)

For generation of photons with these energies by standard SASE schemes geometrical slice emittance of the electron beam at the entrance to the undulator may be estimated as:

$$\varepsilon = \frac{\lambda}{4\pi} \text{ or } \varepsilon_n = \frac{\beta\gamma\lambda}{4\pi}$$

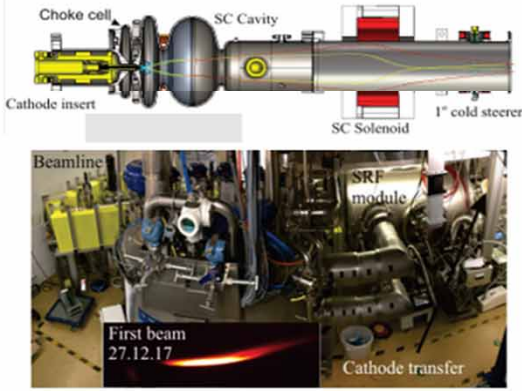
$\varepsilon_n = 1.9 \text{ mm} \cdot \text{mrad}$ for generation of 100 eV photons with 1 GeV beam energy and

$\varepsilon_n = 0.078 \text{ mm} \cdot \text{mrad}$ for generation of 20 keV photons with 8 GeV beam

Bunch charge	100-300 pC	Peak current	3 kA
Bunch repetition rate	1+ MHz	RMS energy spread	$\leq 1.0 \cdot 10^{-4}$
Average current	0.3+ mA		



SRF L-band photocathode gun, HZB

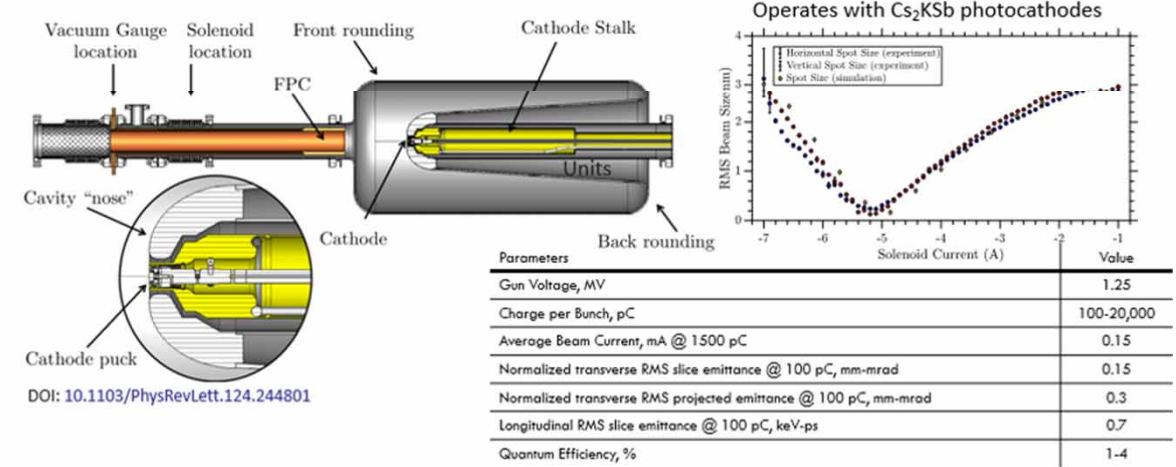


doi:10.18429/JACoW-IPAC2018-TUPML053

B.L. Millitsyn, FLS2023, Lucerne, Switzerland, 28.08-01.09

24

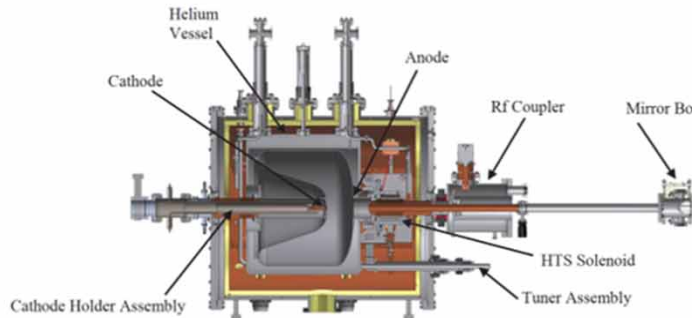
SRF Quarter Wave photocathode gun, BNL



B.L. Millitsyn, FLS2023, Lucerne, Switzerland, 28.08-01.09

25

Wisconsin SRF gun. Design



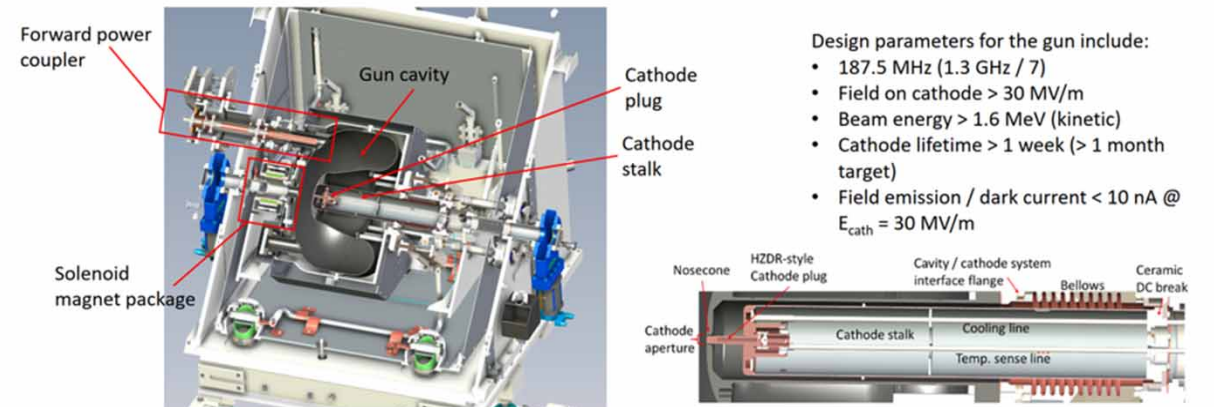
R. Legg et al. IPAC2012, MOPPP045

B.L. Millitsyn, FLS2023, Lucerne, Switzerland, 28.08-01.09

26

Cavities for operation with Cs₂KsB photocathodes

Quarter wave cavity SRF gun



J.W. Lewellen, NAPAC2022, WEP A03

B.L. Millitsyn, FLS2023, Lucerne, Switzerland, 28.08-01.09

27

Potential normalized slice emittance of the RF guns

Photocathode gun technology	Operation mode	Photoinjector operational frequency, MHz	Cathode field, MV/m	Emission pulse length, ps	Normalised beam emittance, nm·rad at bunch charge, pC**			
					20	50	100	300
DC*	CW	DC	10	149.34	28.1	51.8	82.3	171.1
Q-wave SRF	CW	112	20	248.02	10.0	18.5	29.3	61.0
Q-wave NCRF	CW	186	20	149.34	14.1	25.9	41.1	85.6
Q-wave NCRF	CW	186	30	149.34	9.4	17.3	27.4	57.0
Q-wave SRF	CW	217	30	128.01	10.4	19.1	30.4	63.2
L-band SRF	CW	1300	40	21.37	25.7	47.4	75.2	156.4
L-band NCRF	Train-pulsed	1300	60	21.37	17.1	31.6	50.1	104.3
S-band NCRF	Pulsed	3000	100	9.26	18.0	33.1	52.5	109.3
C-band NCRF	Pulsed	6000	200	4.63	14.3	26.3	41.7	86.7

* - injector with DC gun and 186 MHz buncher

** - injection at maximum field

Femtosecond Synchronization of Large Scale FELs

– Achievement, Limitations and Mitigation Paths –

FLS 2023

Holger Schlarb on behalf of the LbSync, Special Diag. and LLRF team at DESY
Lucerne, Switzerland, 30th of August 2023

Introduction

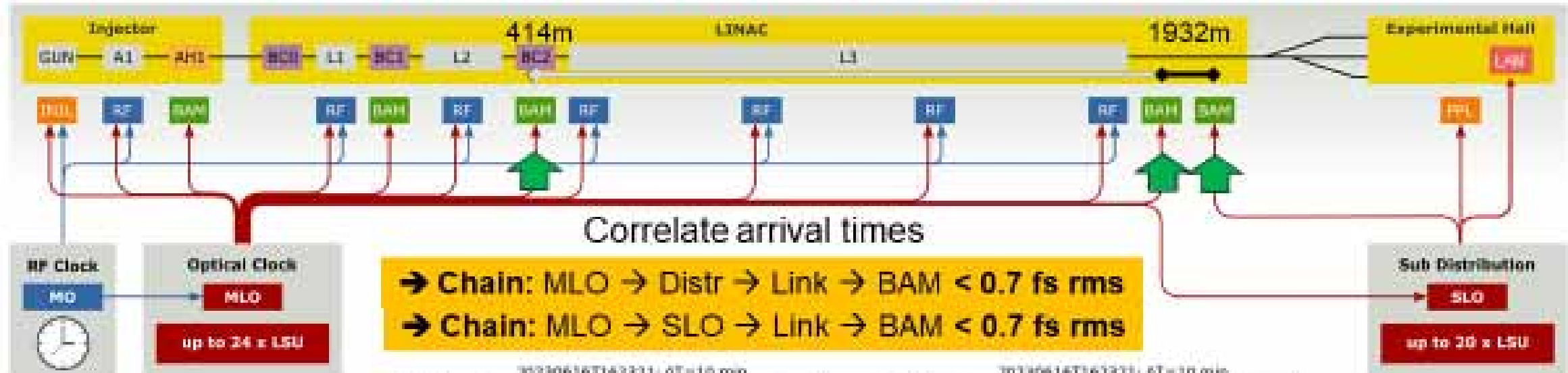
Time & length scales:



Duration matters!

Short range	1us ... 1ms:	PS, EMI, Electronics, Material Prop., ...
Mid range	1ms ... 10s:	Acoustic, Seismic, Air/Water flow, Fans, ...
Long range	10s ... days:	Thermal, Humidity, Air Pressure, ...

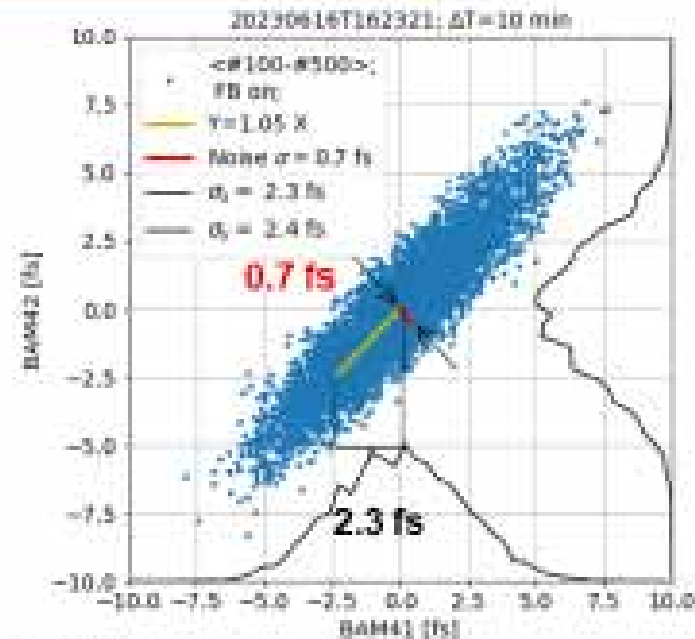
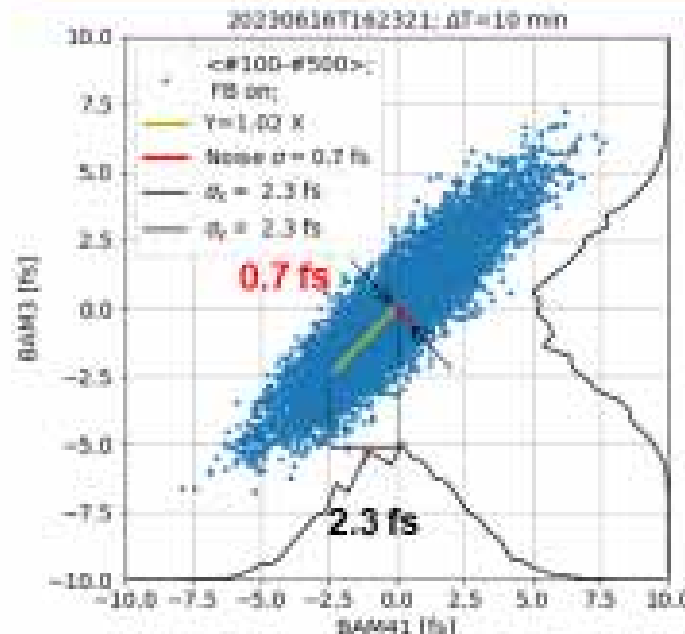
Evaluation of optical synchronization system: - mid range -



10 min. (6000 trains)
mean(400 bunches)

→ Remove BAM high-freq. instr. noise

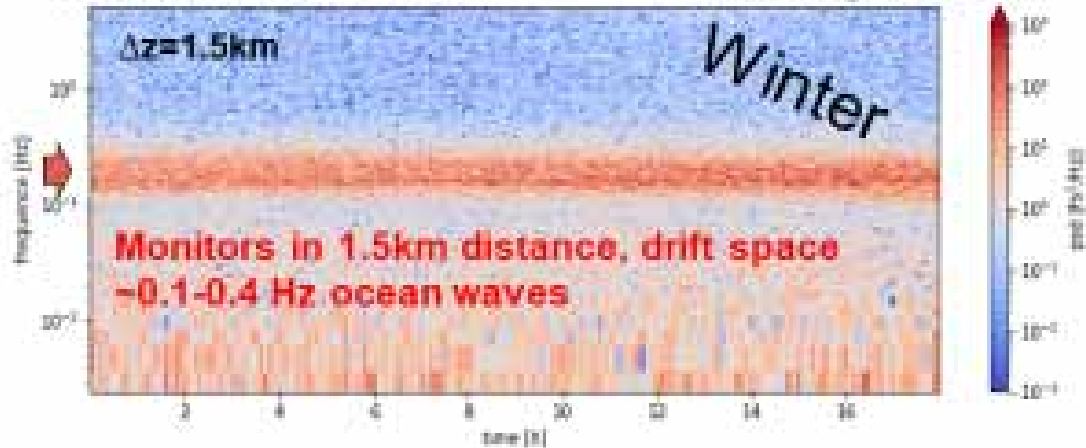
→ Residual jitter of macro-pulses



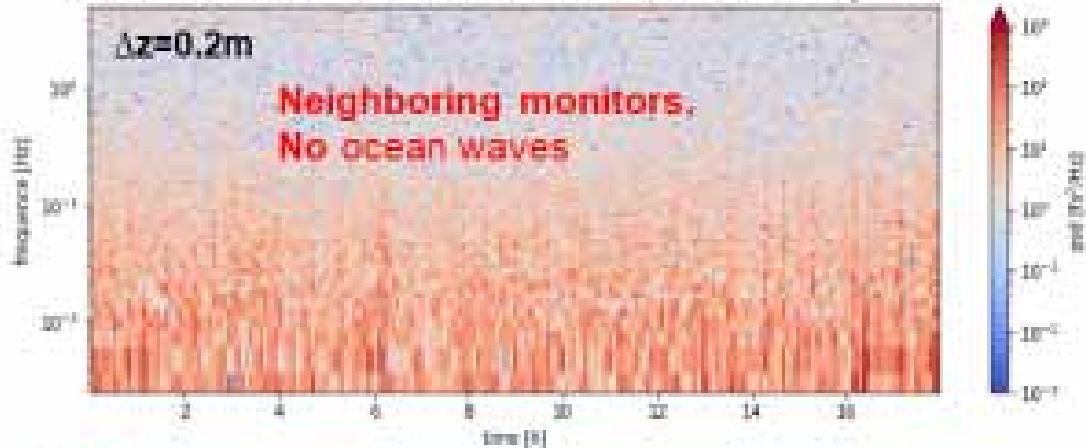
Ocean wave effecting beam arrival

Detection of ocean waves in electron bunch straight path

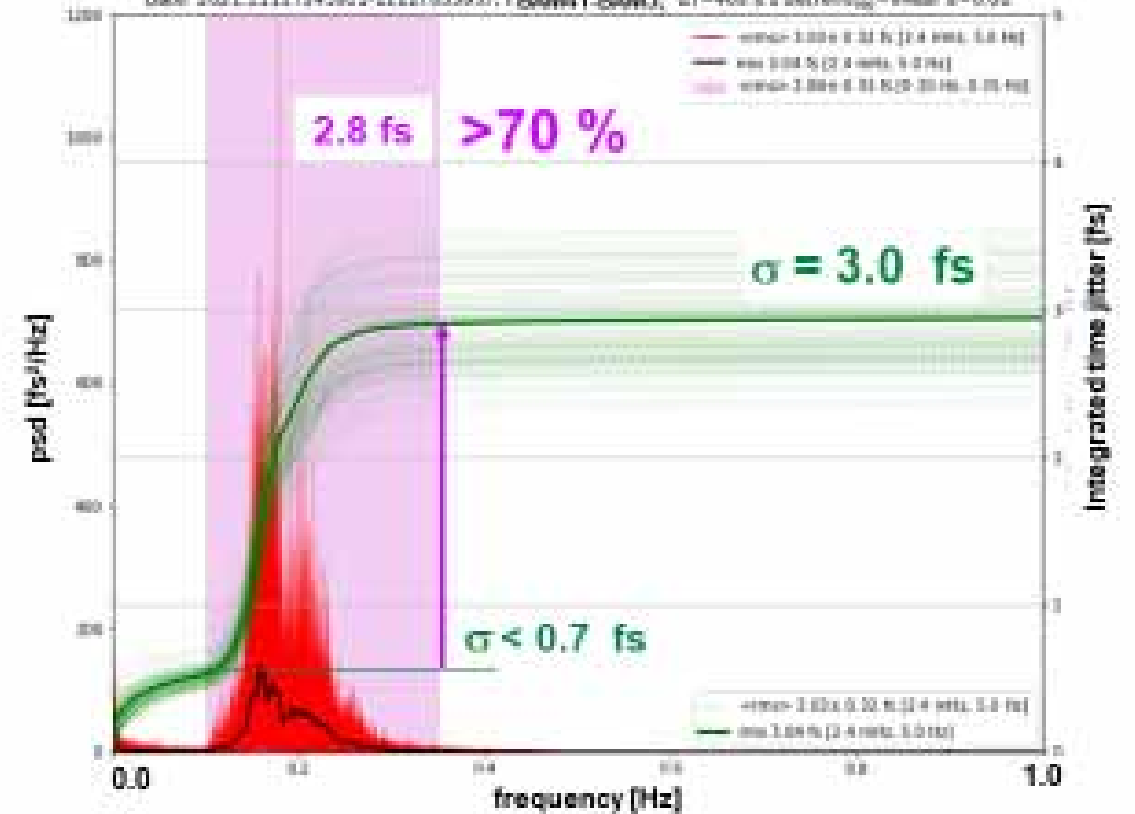
Date: 2021.1111T145951-1112T055957; Data: BAM01-BAM03; T=409.6s; detrend_{avg}=lin a=0.00



Date: 2021.1111T145951-1112T055957; Data: BAM02-BAM04; T=409.6s; detrend_{avg}=lin a=0.00

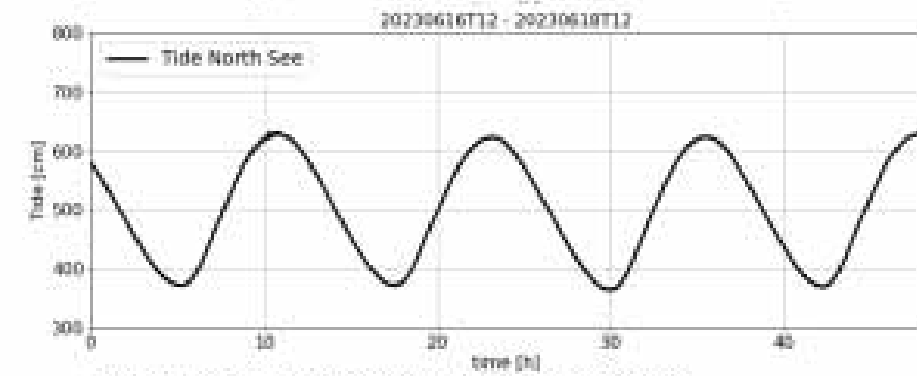
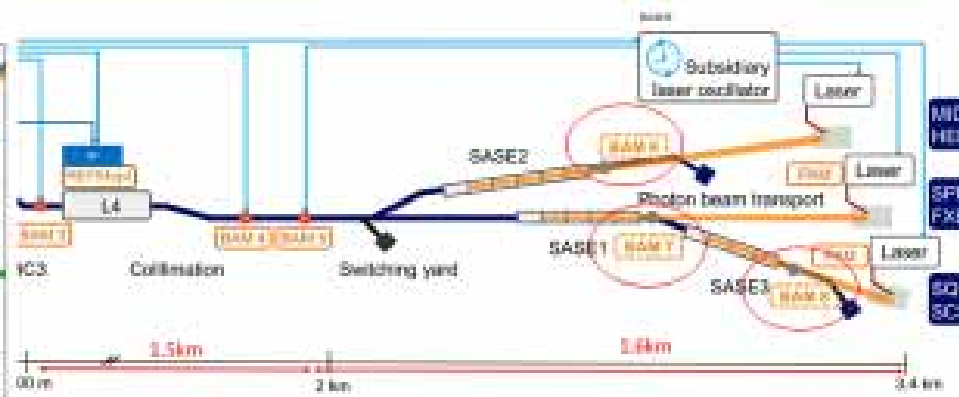
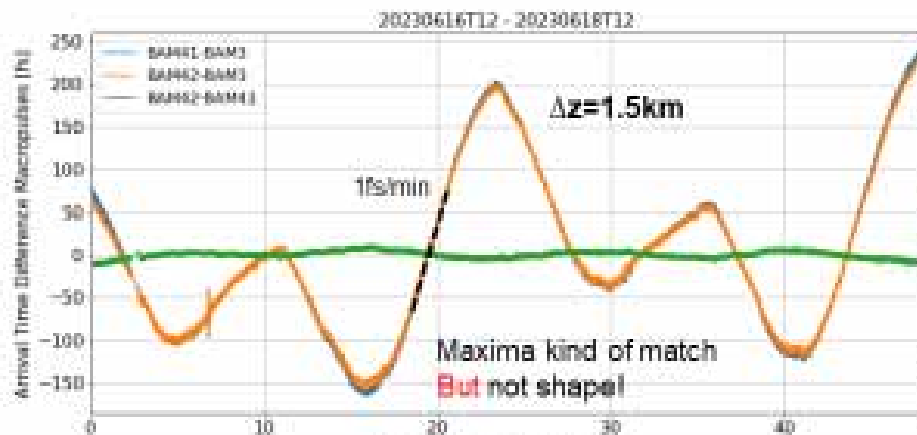


Date: 2021.1111T145951-1112T055957; Data: BAM01-BAM03; T=409.6s; detrend_{avg}=linear a=0.02



Impact of Earth & Ocean Tide

Combined effect earth & ocean tides



Tide data source: www.pegelonline.wsv.de

Mitigation path:
Slow but large variation → precise prediction

- 1) Add new BAM's behind SASE Undu.
- 2) Exp. monitor of tide effect @ DESY side
- 3) Numerical modelling

Conclusion & Outlook

Control jitter and drifts of pump-probe lasers..

- ~1 fs stability MHz – mHz seems feasible, but controlling drifts will be tuff!
- microstructure for as pulse generation → Photon Arrival Monitoring increased relevance

Advanced Electron Beam Diagnostics for FELs

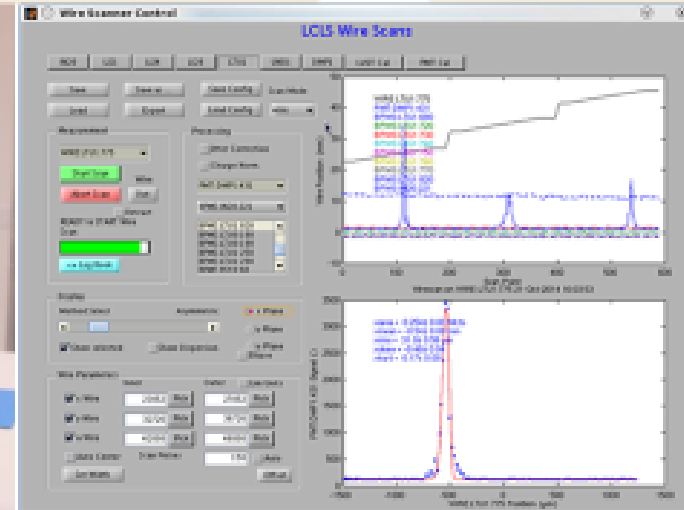
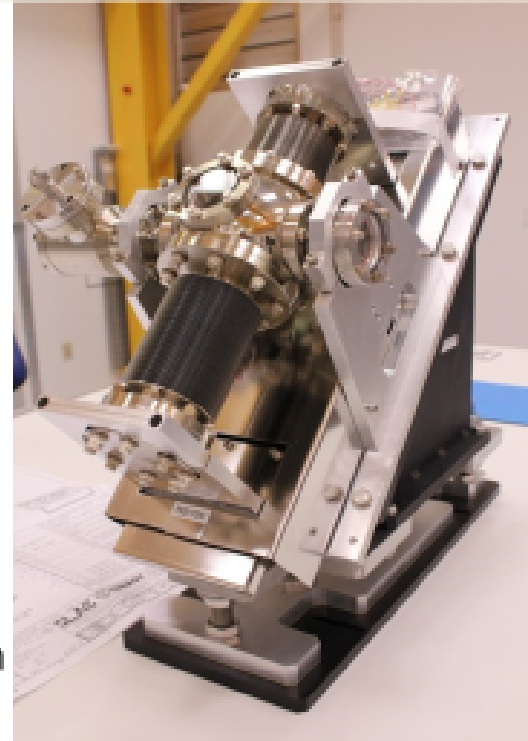
Patrick Krejcik
SLAC



SLAC LCLS Fast Wire Scanner

SLAC

- Fast $\sim 0.5\text{ms}^{-1}$ scanning speed
- At 1 MHz rep. rate ~ 100 bunches intercepted while scanning a $50\ \mu\text{m}$ beam
- $12.5\ \mu\text{m}$ Al:Si wire
- Vibration free operation
- High resolution ~ 1 micron wire position read-back
- Beam synchronous acquisition of wire position during scan together with BLM signal

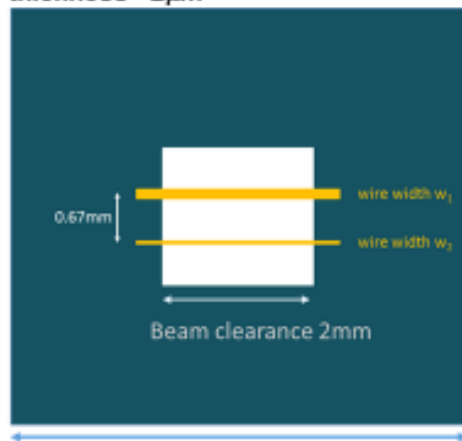


Nano wires for sub-micron emittance – G. L. Orlandi PSI

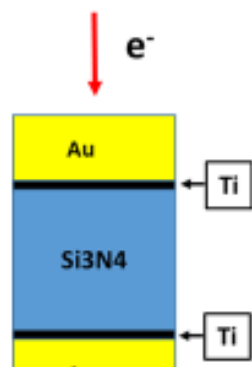
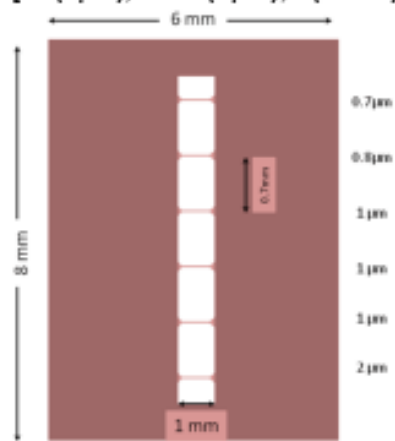
SLAC

- PSI and FERMI are collaborating on nanofabrication techniques for sub-micron wires:

PSI **free-standing** WS chip: bulk Au stripe; width 800nm and 500nm; thickness $\sim 2\mu\text{m}$

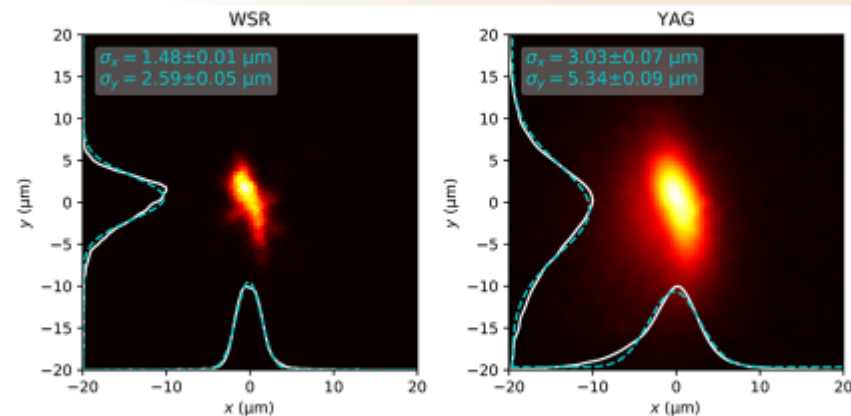


FERMI WS chip: **sandwich** Au/Si3N4/Au; thickness $\sim 3\mu\text{m}$
[Au(1 μm), Si3N4(2 μm), Ti(20nm)]



Beam Measurements of Nanowires vs. YAG Screen

SLAC



Same machine settings for WSR and YAG measurement, charge: 1 pC.

- Streaking with a **RF deflecting structure** reveals the full longitudinal phase space and slice emittance
- Placed down stream of the undulator also reveals lasing temporal profile in the FEL (XTCAV)
 - Temporal resolution can be very good ~ 1 fs
 - But, expensive, limited to ~ 120 Hz operation and subject to phase jitter
- **Passive wakefield deflectors** can have similar resolution
 - Not limited in rep. rate, not subject to jitter, relatively inexpensive
 - But, nonlinear response only kicks the tail of the bunch
 - Also useful for two-bunch, two-color pump probe experiments

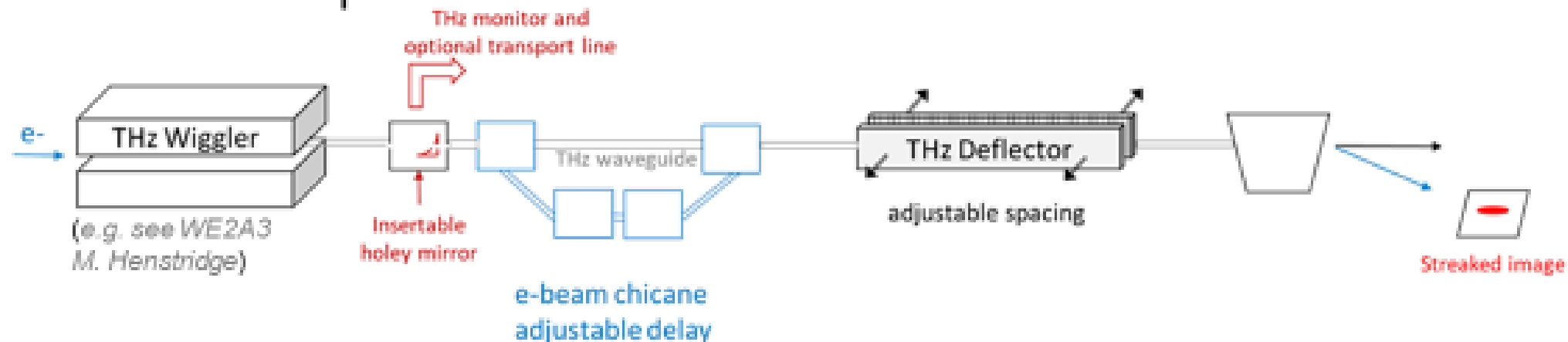
Resolution limits for powered deflectors (e.g. XTCAV)

- **The LCLS XTCAV** resolution is limited to ~ 1 fs because of RF phase jitter from the klystron
 - RMS phase jitter of 0.05° X-band is adequate for operation, but a 0.5° flyer pulse will kick the beam out of its aperture and trip the beam loss monitors, interrupting user operation.
 - As a result we keep the drive power below its maximum amplitude
- **A next-generation deflector with attosecond resolution** must address three issues simultaneously
 1. The wavelength must be considerably shorter in order to increase the "streak" dV/dt
 2. A high-power source must be available at the chosen wavelength
 3. The power source must be phase locked to the beam

SLAC Proposal for a Beam-Synchronous THz Deflector

SLAC

- SLAC LDRD proposal P. Krejcik, V. Dolgashev, A. Fisher, D. Nguyen
- Exploit the spent FEL electron beam to make a high-power wiggler-based THz source that is inherently synchronous with the beam, and at the same repetition rate.



Variable chicane delay adjust the phase between the electron bunch and the THz deflecting field.

Planar deflecting structure with variable spacing to allow large beam stay-clear during setup.

Beam Diagnostics for Ultra-Low Emittance Storage Rings



Overview of LESR Diagnostics Systems

Parameter	Measurement System	Status / Remark
Beam Current *	ICT & DCCT	ready for LE rings
Filling Pattern *	button pick-up, visible or X-ray diode	ready for LE rings
Bunch Purity *	visible or X-ray APD / TCSPC	ready for LE rings
Bunch Length *	visible light & synchro-scan streak camera	ready for LE rings
Beam Loss *	scintillator & PMT	ready for LE rings
ID & Machine Protection *	scrapers & collimators	ready for LE rings

* These diagnostics systems will not be treated in detail during this presentation. Remarks and examples may be given in additional slides or references.

Beam Position	button pick-ups & BPM electronics	long-term drifts resolution
Tune and Chromaticity *	pinger or stripline kicker & BPM electronics	ready for LE rings
Emittance & Energy Spread	x-ray imaging (pinhole camera) & diffraction visible light interference & pi-polarization	needs improvement, complex engineering
Beam Stability	fast orbit feedback filling pattern (top-up) & coupling feedbacks	increased BW (1 kHz), include X-BPMs
Instabilities, Emittance Control	multi-bunch feedback	implement ϵ -FB, injection transients

LESR / 4GLS Profile Monitors – State-of-the-Art

X-Ray Pinhole Camera

- C. Thomas et al., “X-ray Pinhole Camera Resolution and Emittance Measurement”, Phys. Rev. ST Accel. Beams **13**, 022805 (2010)

π -Polarization Monitor with Diffraction Obstacle

- Å. Andersson, J. Breulin et al., “Transverse Beam Diagnostics at MAX-IV”, I.FAST Workshop, KIT, Karlsruhe, Germany, April 2022 (virtual)

Coded Aperture

- J.W. Flanagan et al., “X-ray Monitor based on Coded-Aperture Imaging for KEKB Upgrade and ILC Damping Ring”, Proc. EPAC 2008, Genoa, Italy, TUOCM02, 1029

Single or Double Slit Interferometry

- T. Naito, T. Mitsuhashi, “Very Small Beam size measurement by a Reflective Synchrotron Radiation Interferometer”, Phys. Rev. ST Acc. Beams **9**, 122802, December 2006
- M. Masaki, S. Takano, “Two-Dimensional Visible Synchrotron Light Interferometry for Transverse Beam Profile Measurement at the Spring-8 Storage Ring”, Journal of Synchrotron Radiation **vol. 10, part 4**, July 2003, 295-302

Fresnel Zone Plates

- H. Sakai et al., “Improvement of Fresnel Zone Plate Beam-Profile Monitor and Application to Ultralow Emittance Beam Profile Measurements”, Phys. Rev. ST Acc. Beams **10**, 042801, April 2007

X-Ray Diffraction

- B. Yang, S. Lee, “Planned X-Ray Diffraction Diagnostics for APS-U Emittance Measurements” ARIES Topical Workshop on Emittance Measurements for Light Sources and FELs, Barcelona, Spain, January 2018
- N. Samadi et al., “A Spatial Beam Property Analyzer Based on Dispersive Crystal Diffraction for Low Emittance X-Ray Light Sources”, Scientific Reports **12**, 18267 (2022)

ARIES Topical WS on Emittance Measurements for Light Sources & FELs

technique	measured σ
X-ray pinhole camera	7 μm
comp. refractive lenses	10 μm
visible light interferometry	3.9 μm
π -polarization	3.7 μm
coded aperture	5 μm
X-ray diffraction	4.8 μm
X-ray interferometry	4.8 μm

<https://indico.cells.es/event/128/overview>

ALBA, Barcelona, Spain January 2018



Photon Beam Position Monitors

Different types of photon BPMs have already been successfully used at many **3GLS**

- ID gap calibration (with blade monitors and GRID XBPMs in front end)
- beamline alignment (using CVD sc-diamond or SiC quad detectors)
- providing mainly slow photon beam position feedbacks (drift compensation)



Photon BPMs – FB Integration at 4GLS I

In many **3GLS**, Photon BPMs are important devices for beamline stabilization but most of them are not yet part of a fully integrated beam stabilization concept

For **4GLS DLSR**, we should use the potential of Photon BPMs even better...

- examination and elimination of **systematic effects** (e.g. radiation background)
- developing and following **new monitor and sensor concepts**
- **synchronized DAQ and common FB platform** with electron BPMs (FB or watchdog)
- **responsibility** for electron and photon BPMs in "one hand" ...???

Application of Superconducting Undulator Technology for Hard X-ray Production at European XFEL



Johann E. Baader
*Undulator Scientist at
European XFEL*

Future Light Sources
Workshop (FLS23)
August 31st, 2023

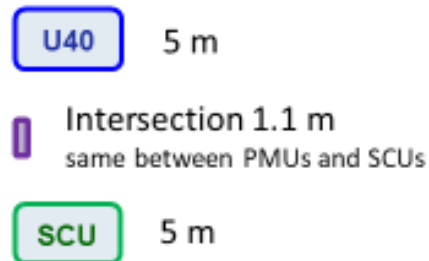
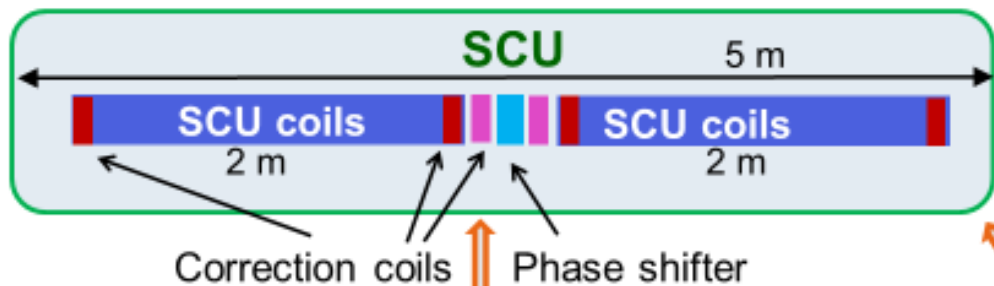
FESTA: the SCU afterburner planned for EuXFEL



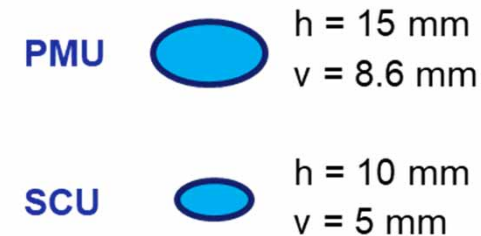
+



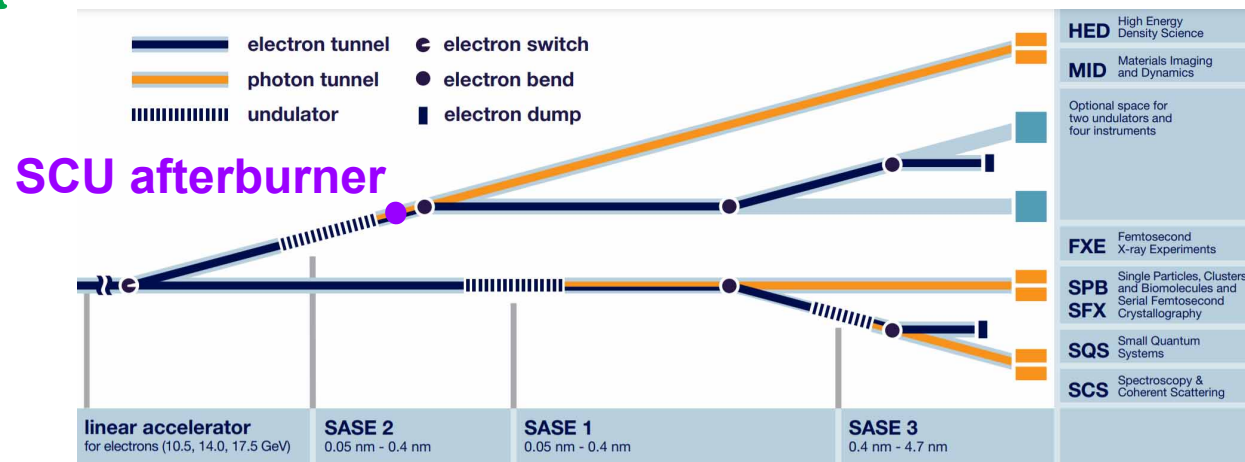
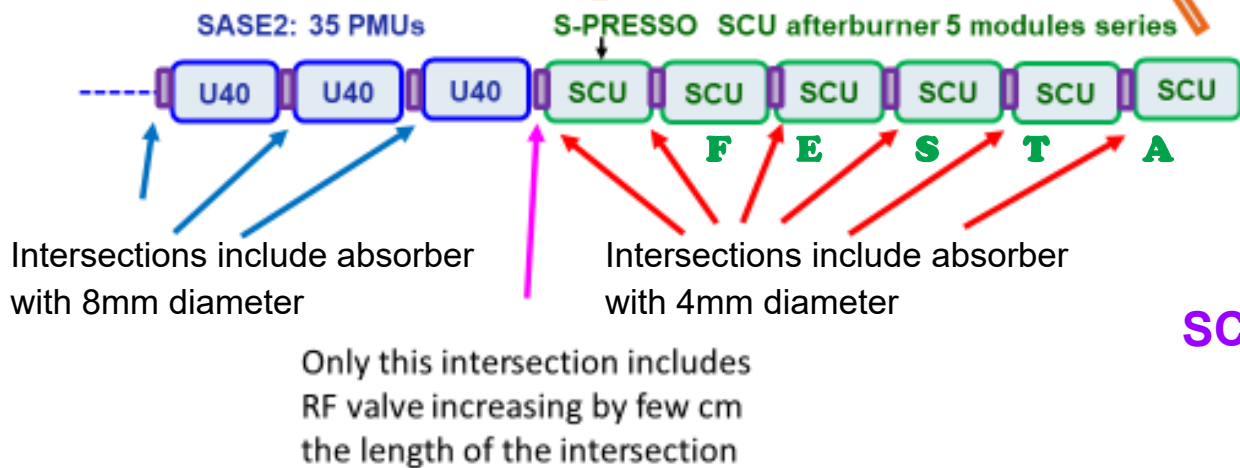
Cryostat



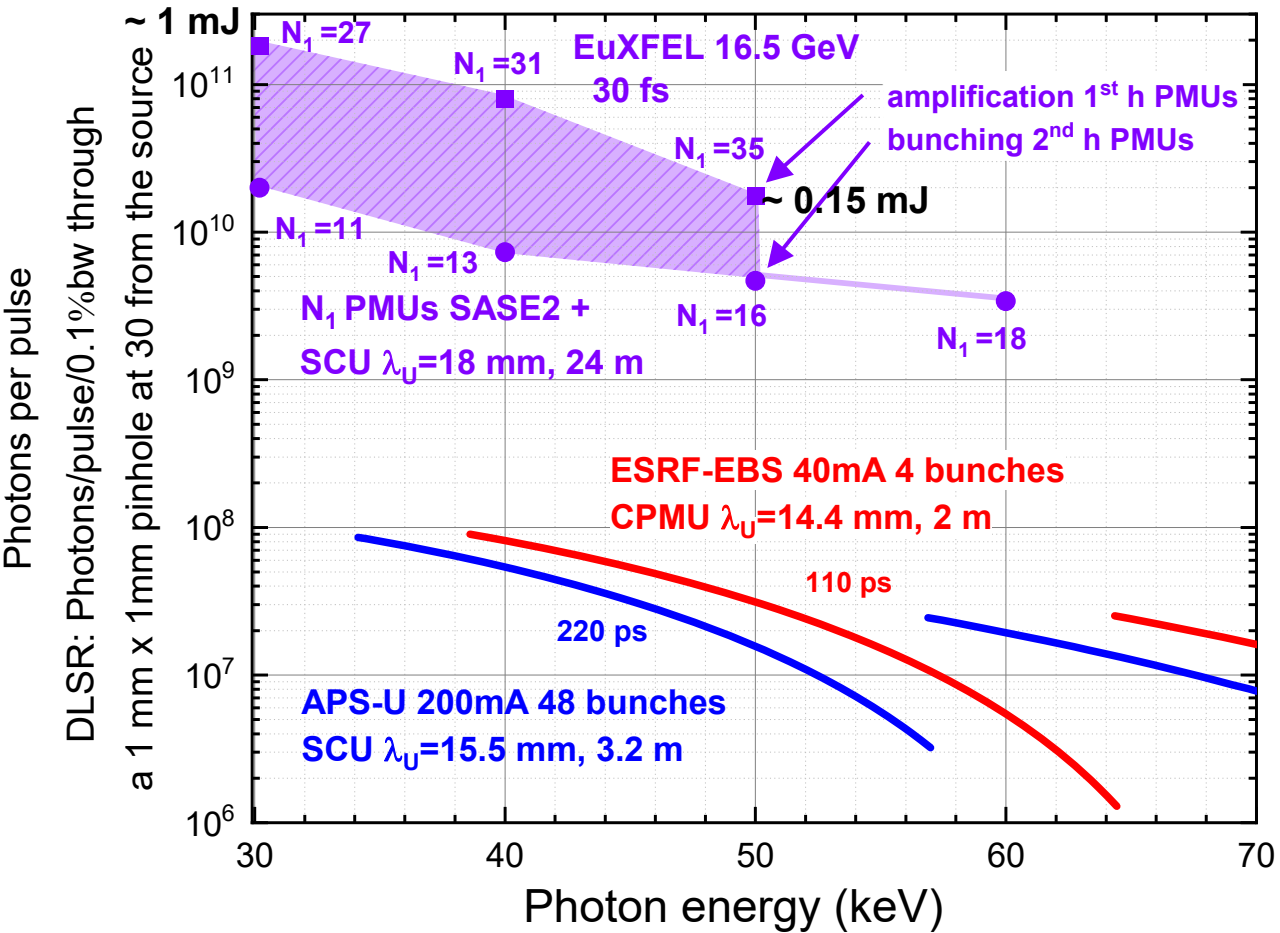
Cross section vacuum chamber



The cooling scheme of all modules will be based on **cryocoolers** as from the KIT/Noell design



FESTA: the SCU afterburner planned for EuXFEL



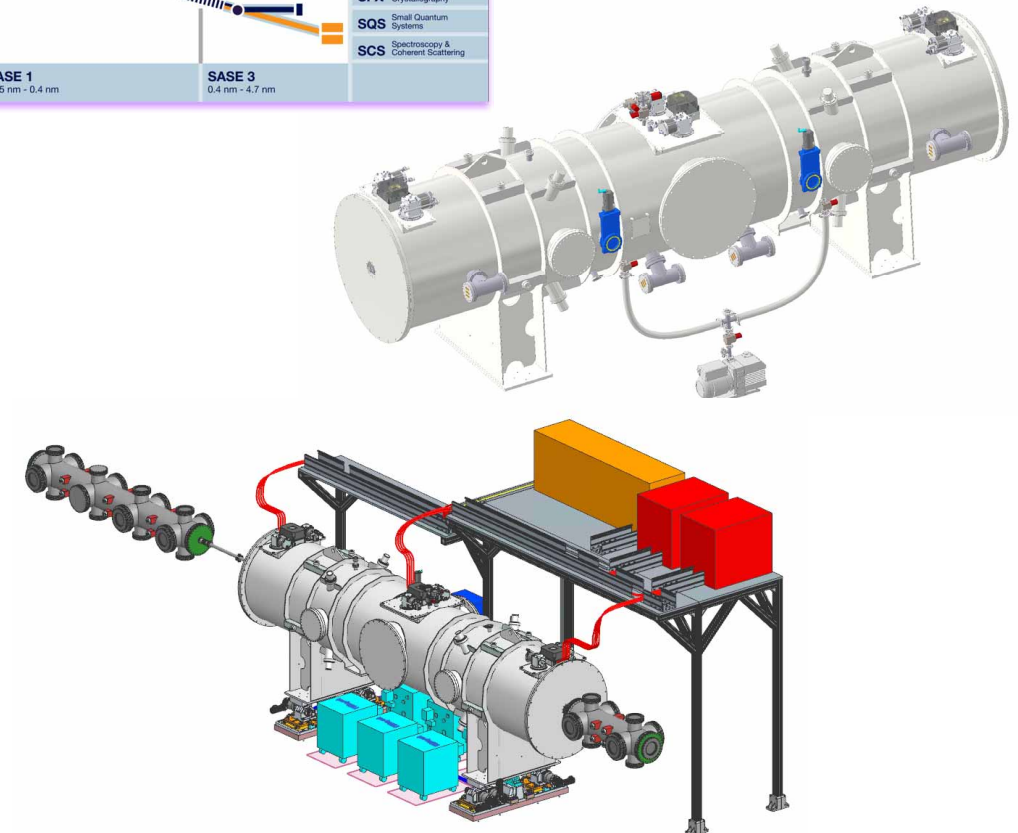
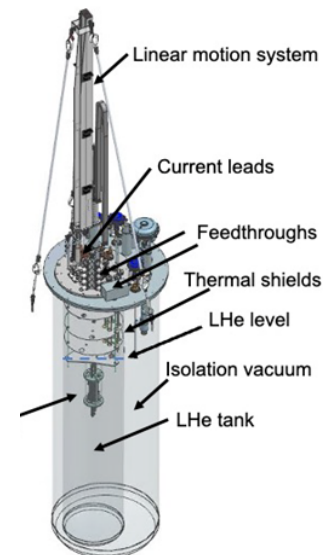
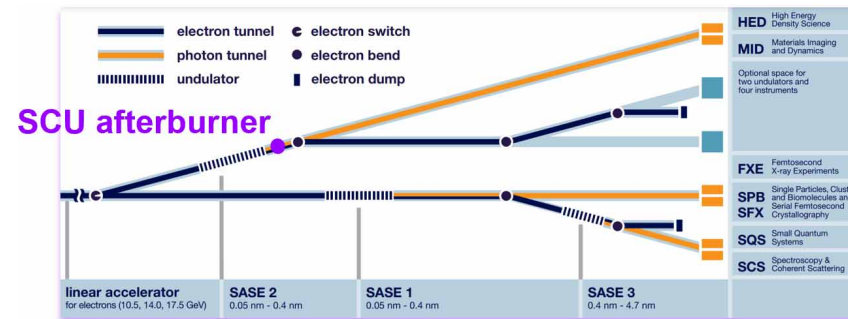
Normalized emittance	0.4 mm mrad	The simulations do not consider wake fields and tapering. A flat top 3 fs bunch is considered
Initial energy spread	3 MeV	
Current	5 kA	

Estimated range of photons per pulse achievable by tuning the SCU afterburner on the fundamental

- amplifying the output of the fundamental of the PMUs
- using the bunching of the second harmonic of the PMUs
- More detailed studies considering wake-fields, tapering, 'real' bunch distribution and optimized electron bunch properties are ongoing

In summary, EuXFEL aims to demonstrate the operation of SCUs in X-Ray FELs

- Benefits: CW mode; potential to lase at higher photon energies (>40 keV)
- SCU afterburner is planned
- The first module S-PRESSO has been specified, the contract assigned to Bilfinger Noell GmbH, the TDR received and production has started
- Complex tunnel integration is ongoing, and all points are addressed and are on track
- Two test facilities to characterize SCU coils and SCU undulators are under development
- R&D on advanced SCU coils



Bulk Superconductor and its Application for Insertion Device

Toshiteru KII

Institute of Advanced Energy, Kyoto University



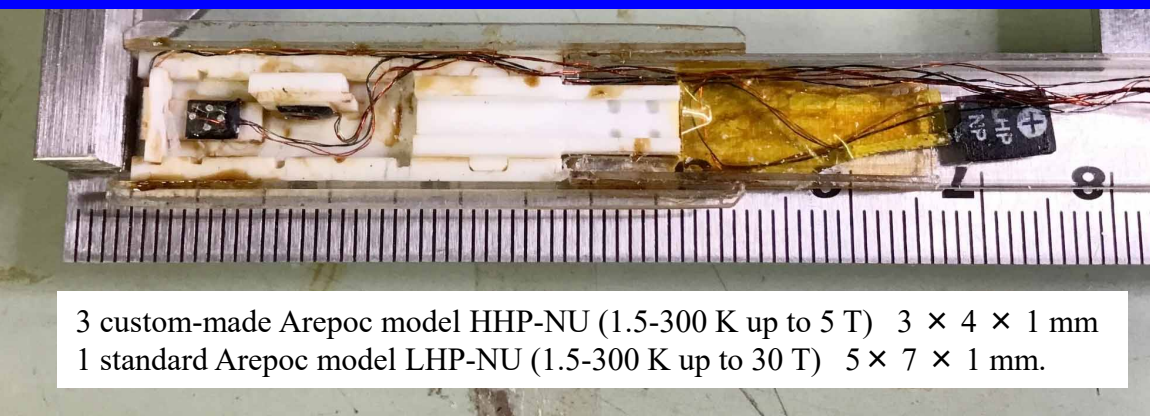
Experimental

Prototype Undulator



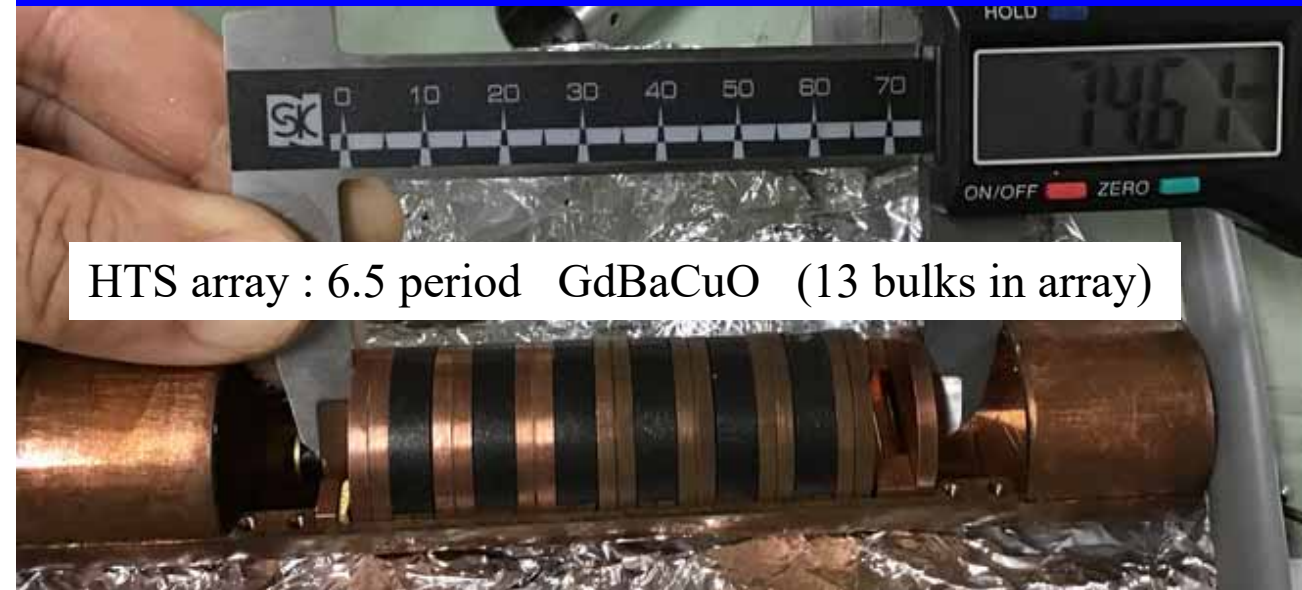
custom 6 T superconducting solenoid
room temperature bore ϕ 10 cm

Hall sensor array



3 custom-made Arepoc model HHP-NU (1.5-300 K up to 5 T) $3 \times 4 \times 1$ mm
1 standard Arepoc model LHP-NU (1.5-300 K up to 30 T) $5 \times 7 \times 1$ mm.

HTS array



HTS array : 6.5 period GdBaCuO (13 bulks in array)

GdBaCuO bulk



Single Domain HTS

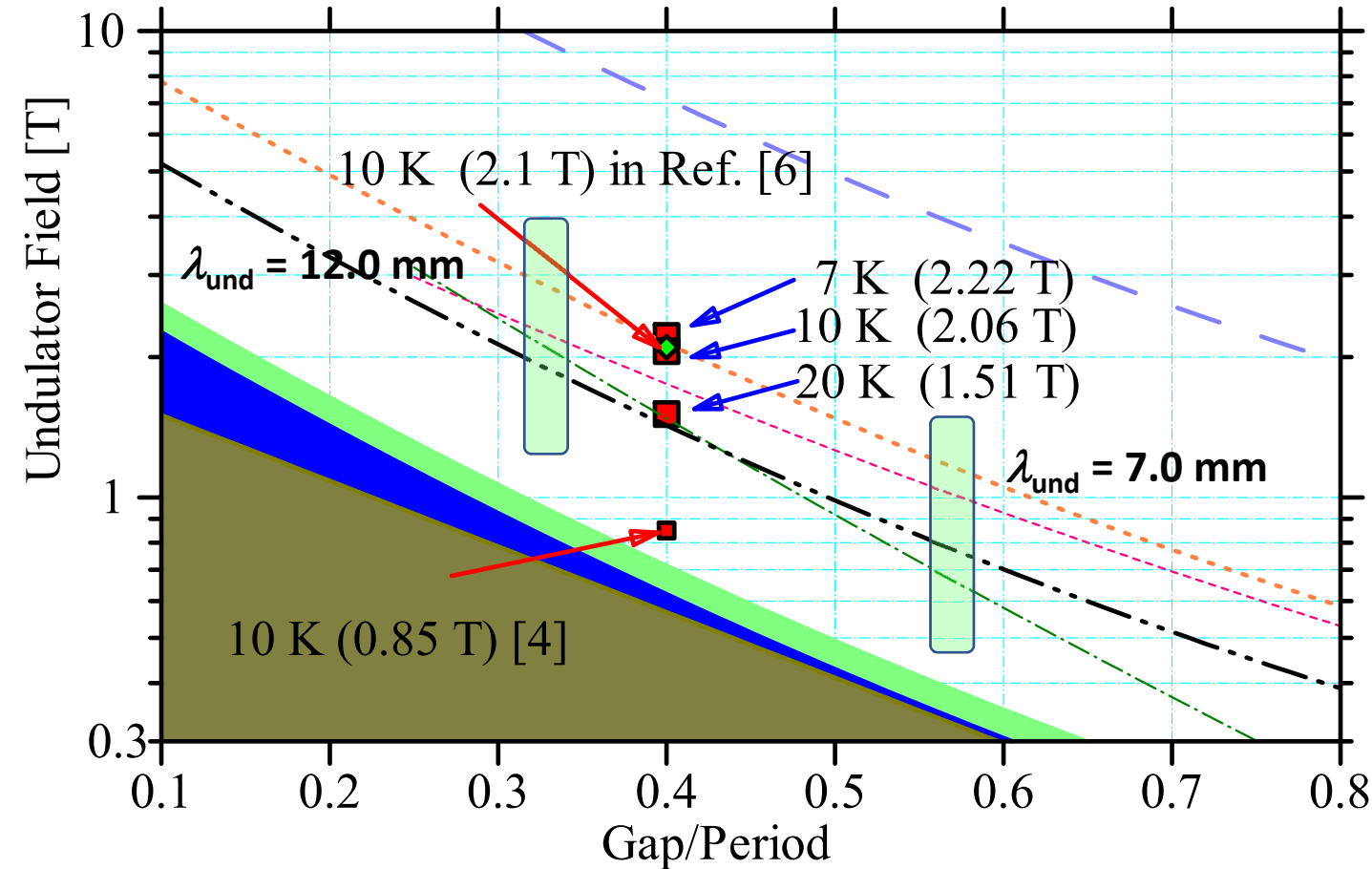
QMG™ by Nippon Steel
GdBaCuO

$T_c \sim 90$ K

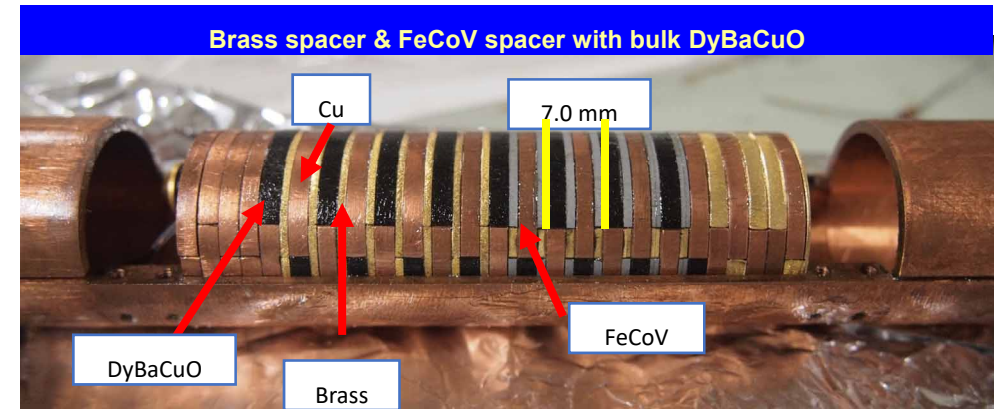
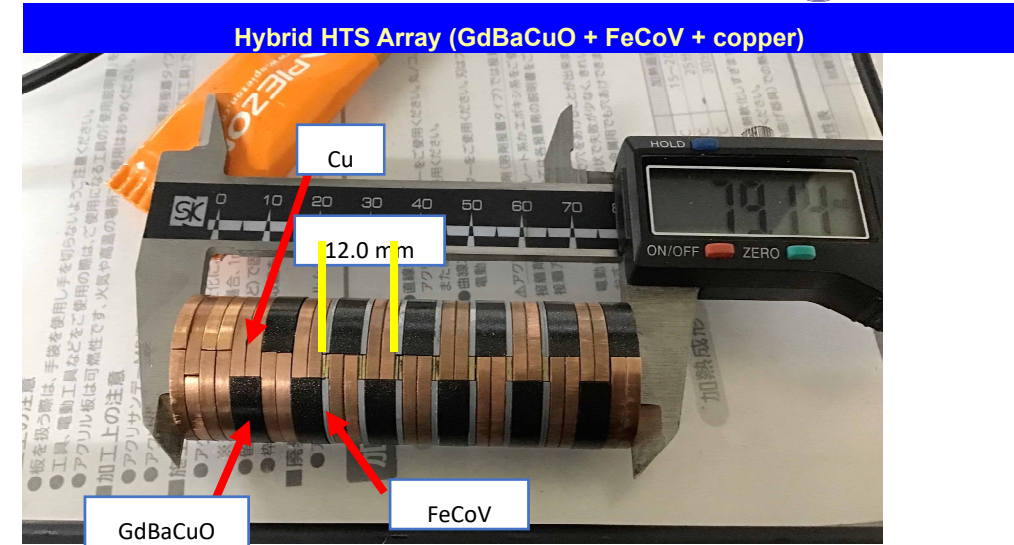
$J_c > 10$ kA/mm² @10 K, 2T



Summary



- Permanent Magnet (PM)
- PM Hybrid
- Cryo PM Hybrid (PM Hybrid ×1.15)
- Superconducting planar (expected)
- Superconducting planar in Ref. [10]
- Bulk HTS SAU This work
- Bulk HTS SAU in Ref. [4]
- Bulk HTS SAU in Ref. [6]
- Cryo PM Hybrid ×2
- Cryo PM Hybrid ×3
- Cryo PM Hybrid ×10



Results for $\lambda_{und} = 7.0, 12.0$ mm with hybrid structure will be unveiled soon.

SCU Development at the LCLS for Future FELs

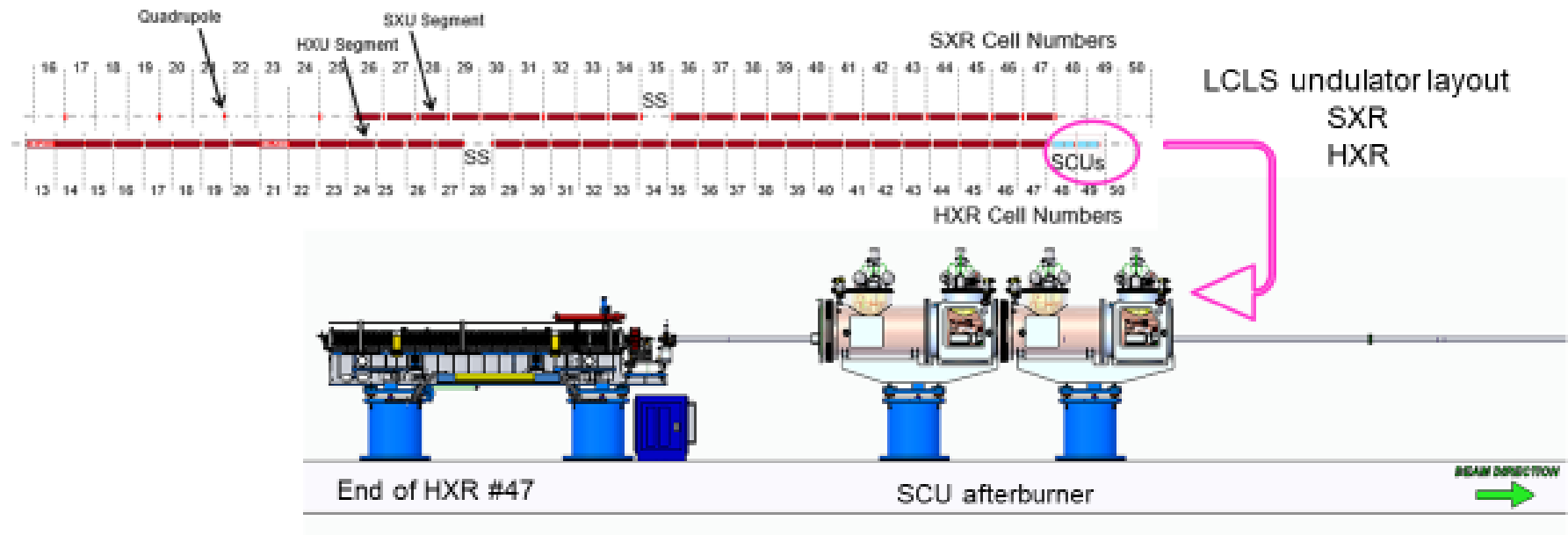


Patrick Krejcik

G. Bouchard, D. Caltabiano, G. Gassner, Z. Huang, E. Kraft, B. Lam, A.M. Montironi, C. Nantista, D.C. Nguyen, H-D. Nuhn, X. Permanyer, Z. Wolf, Z. Zhang, **SLAC**

E. Antliker, J. Byrd, J. Fuerst, E. Gluskin, Y. Ivanyushenkov, M. Kasa, I. Kesgin, M. Qian, Y. Shiroyanagi, **ANL**

SCU Prototype Installation at end of LCLS HXR



- SCU parameters chosen to match FEL resonance of existing HXR undulators
- Cryomodule design will be extendable into a full-length FEL beamline

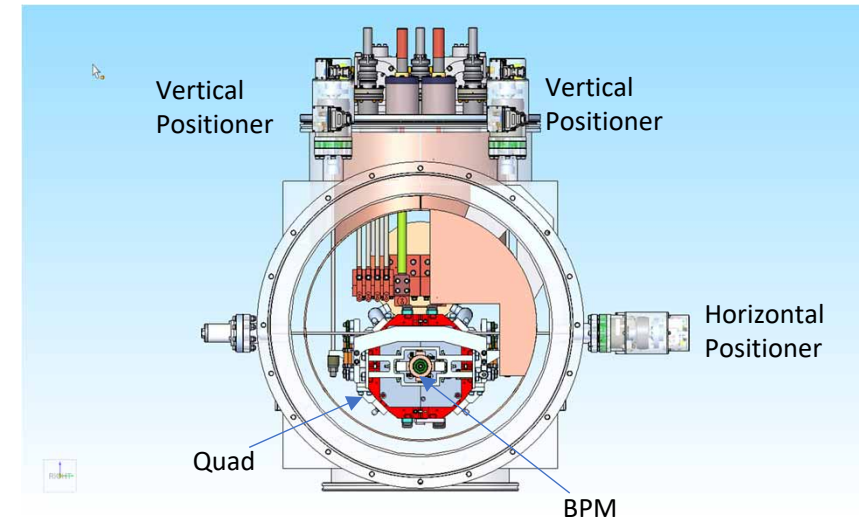
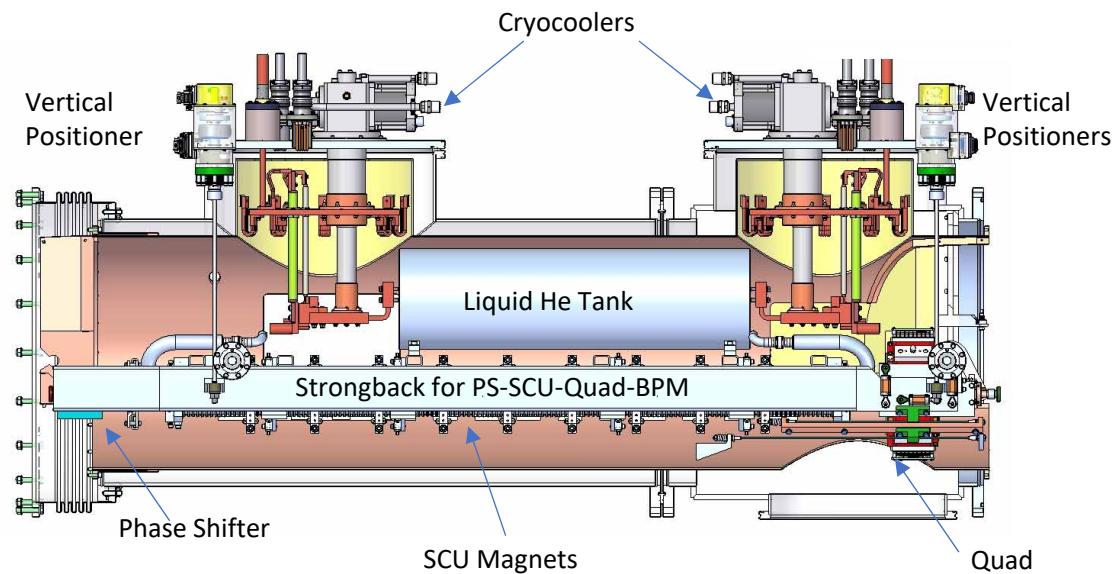
Prototype Design Choices

Superconductor material: NbTi at 4 K (other superconductors will be considered for future FEL testing)

SCU period & polarization: 21-mm period and vertical polarization (matching FEL wavelength of HXUs)

Alignment method: Internal vertical and horizontal position adjustments with linear actuators

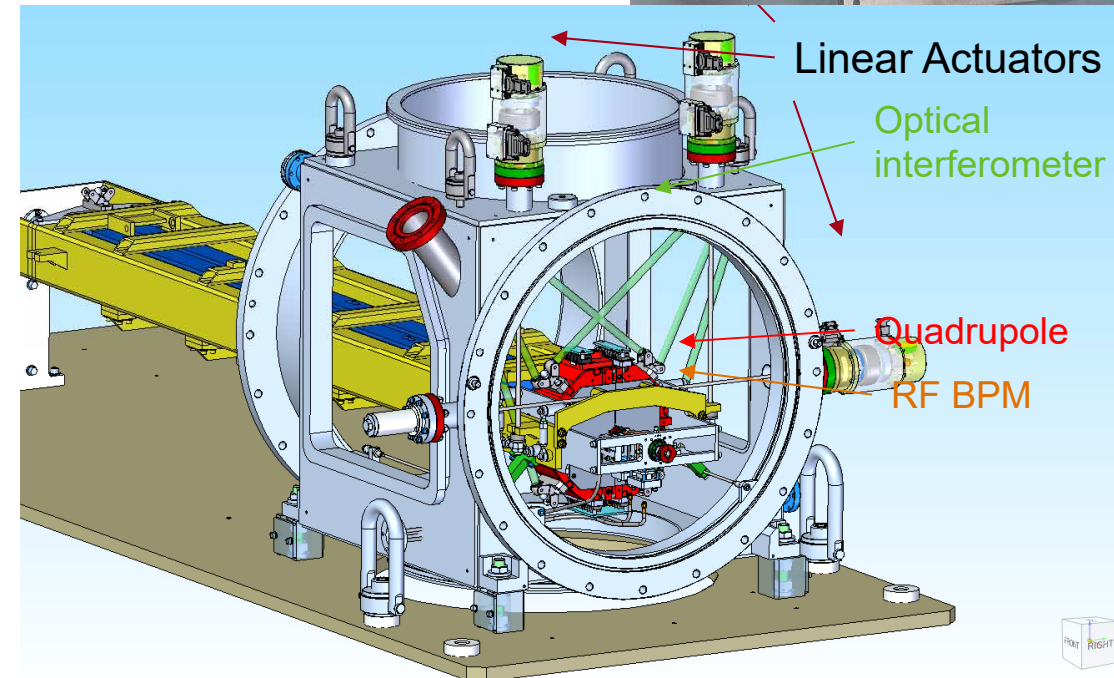
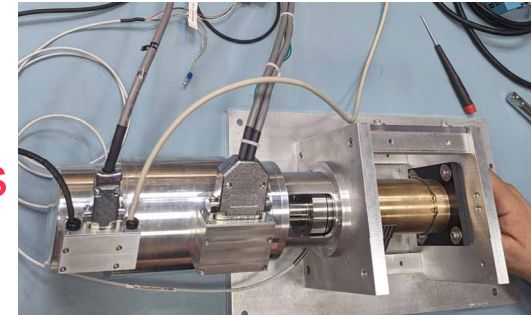
Beamline components: Phase Shifter-SCU Magnets-Quad-BPM, all operate at cryogenic temperature



Current Status of the Project

SLAC

- Completed the design and fabrication of **Precision Alignment Test Stand**
- Phase 1 testing:
 - Flanges and chamber removed for CMM calibration of **linear movers**
 - And set up of internal **optical interferometers**
 - Measurement of vibration modes
- Internal strongback supports the:
 - **undulator cores**, **quadrupole**, **RF BPM**
- The test stand prototypes all the mechanical features of the cryomodule



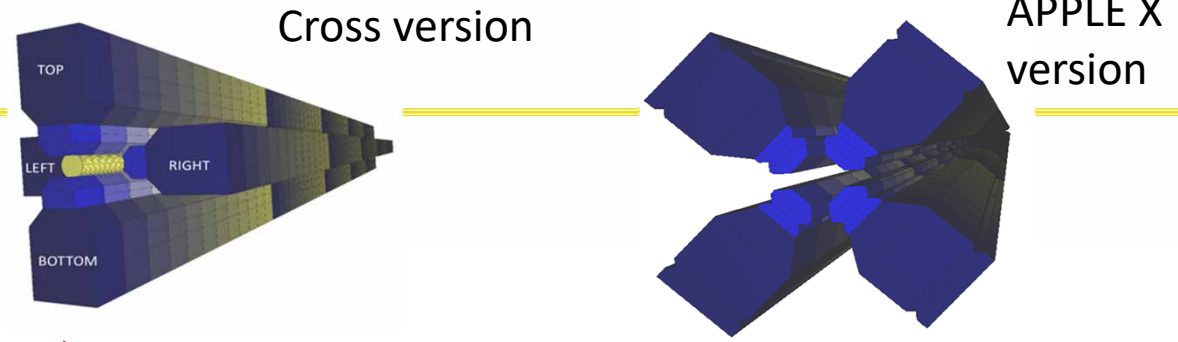
Bi-periodic Undulator: Innovative Insertion Device for SOLEIL II

67th ICFA Advanced Beam Dynamics
Workshop FLS 2023

Angela Potet
Synchrotron SOLEIL, France
(TH1D4)

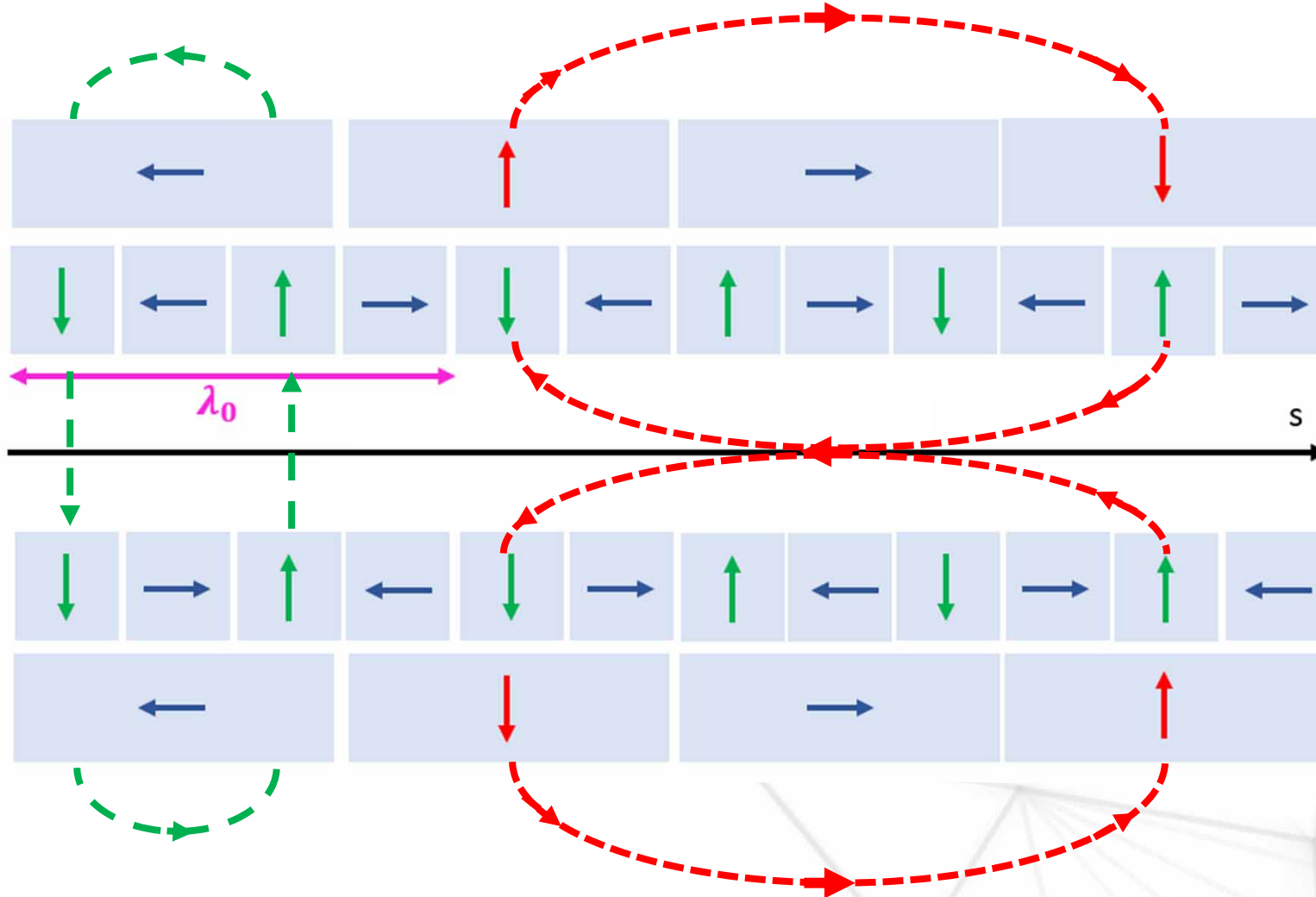
*Frédéric Blache, Pascale Brunelle, Marie-Emmanuelle Couprie, Carlos De Oliveira, Arnaud Mary,
Thibaut Mutin, Amor Nadji, Keihan Tavakoli, Olivier Marcouillé (Synchrotron SOLEIL)*

Principle of operation



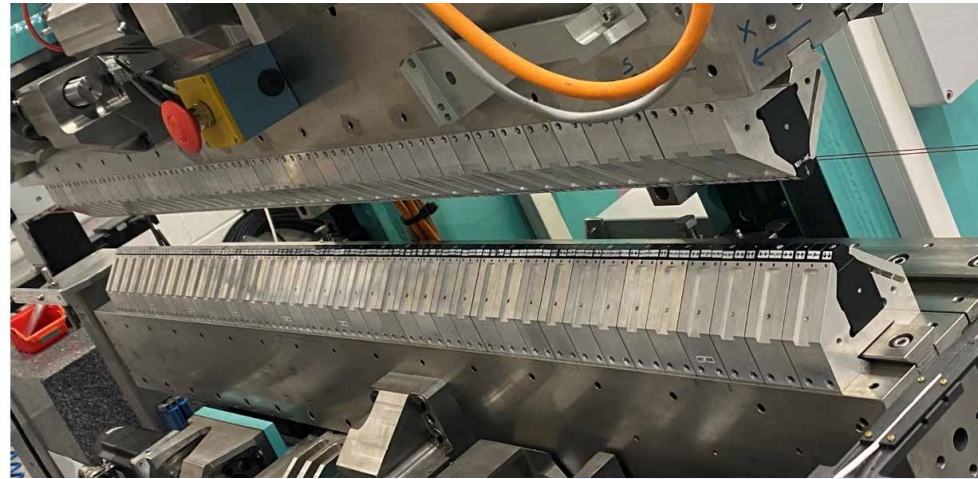
- λ_0 mode:

Field line generated by the magnets of the λ_0 period: Addition of the B_z field on the axis

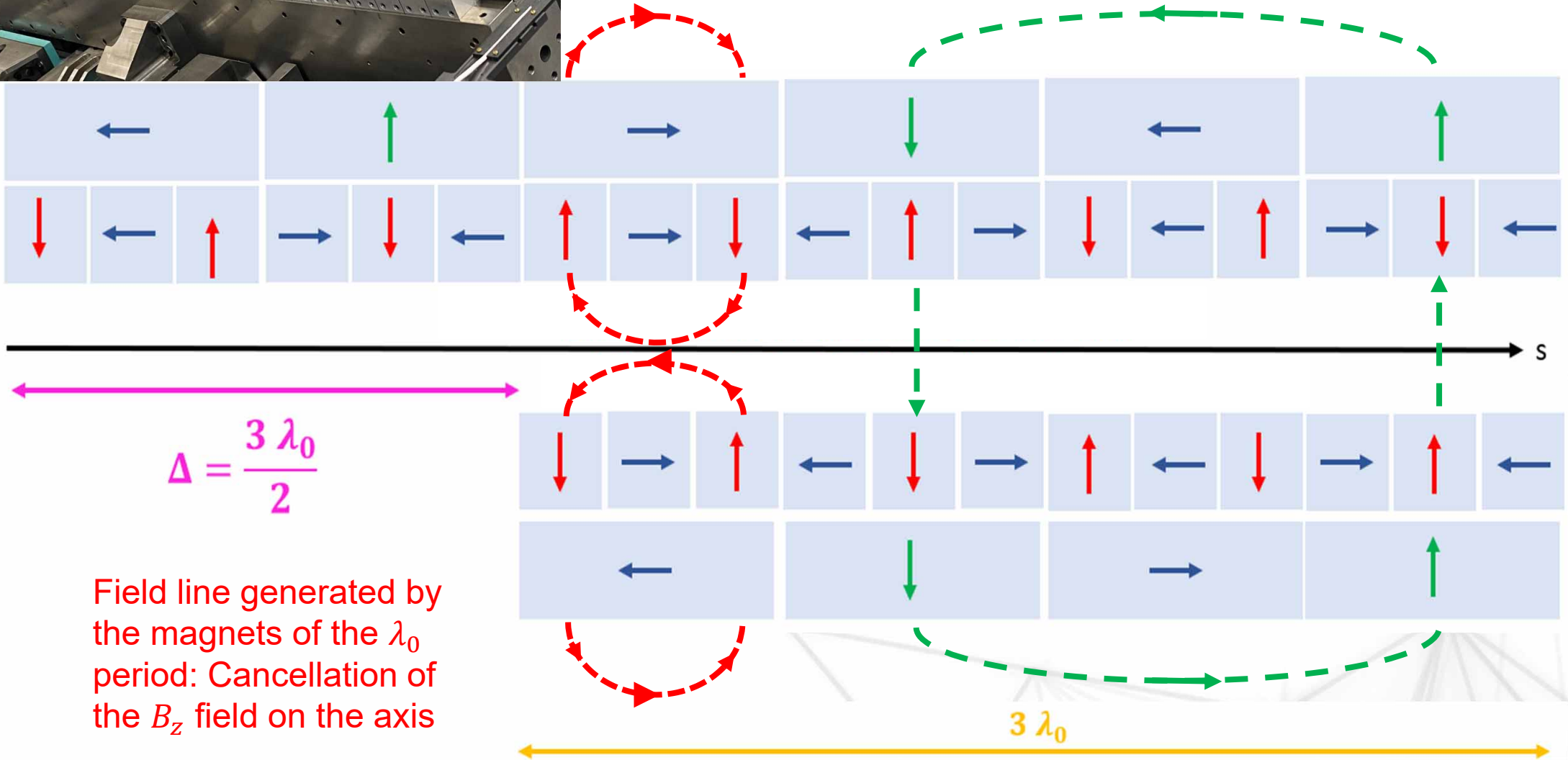


Field line generated by the magnets of the $3\lambda_0$ period: Cancellation of the B_z field on the axis

Principle of operation



Field line generated by the magnets of the $3\lambda_0$ period:
Addition of the B_z field on the axis



Field line generated by the magnets of the λ_0 period: Cancellation of the B_z field on the axis

Beam losses and radiation studies for advanced operation schemes at the European XFEL

Shan Liu, Winfried Decking, Albrecht Leuschner (DESY), Andrew Potter, Andrzej Wolski (The University of Liverpool), Sara Casalbuoni, Suren Karabekyan, Harald Sinn, Frederik Wolff-Fabris (EuXFEL), Frank Jackson (STFC/ASTeC), Junjie Guo (SINAP)

67th ICFA Advanced Beam Dynamics Workshop on Future Light Sources
Lucerne, Switzerland
August 31st 2023

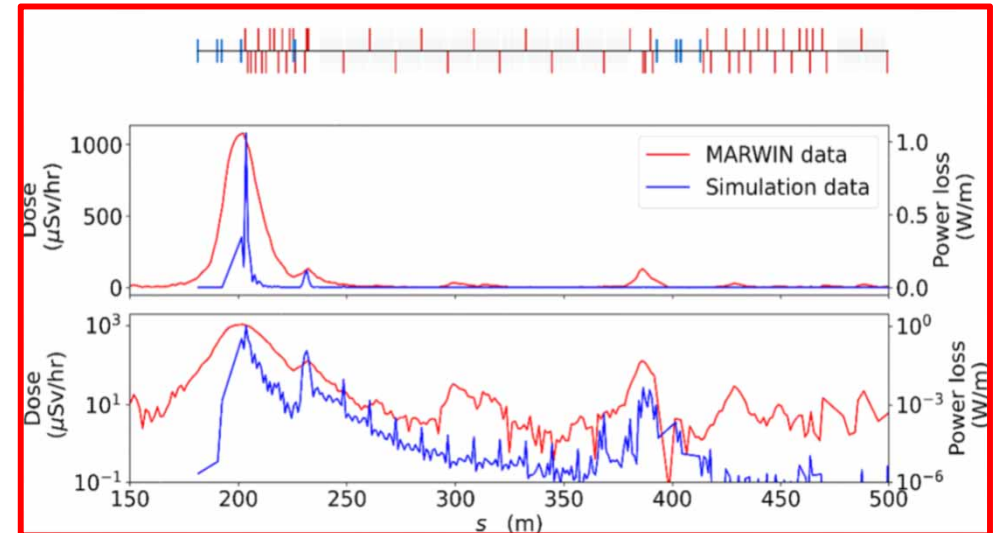


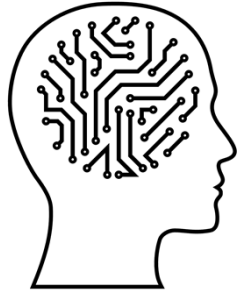
HELMHOLTZ
RESEARCH FOR GRAND CHALLENGES



Why taking care of radiation?

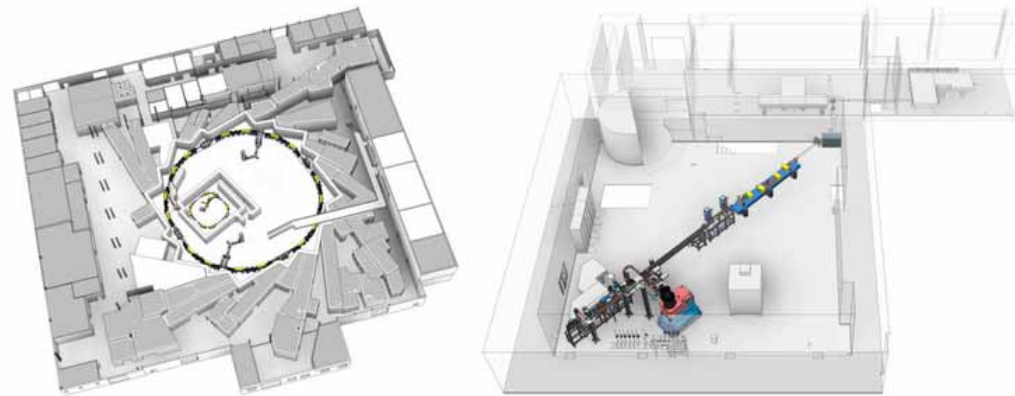
- Damage of équipements
- Damage of ID
 - PM undulators +++
 - SCU: not critical
- Simulation and cross check Slotted Foils and LYSO Screen
- Measurement with Marwin movable robot along the acceleration line: nice agreement
- APPLE-X encoders of FEL damaged
 - Mesurement and search for location
 - Encoder change
 - Installation of protection
 - ID ready for re-installation
 - Lead shielding on the upstream absorber





How can machine learning help future light sources?

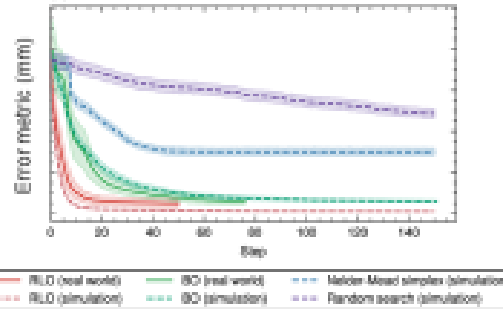
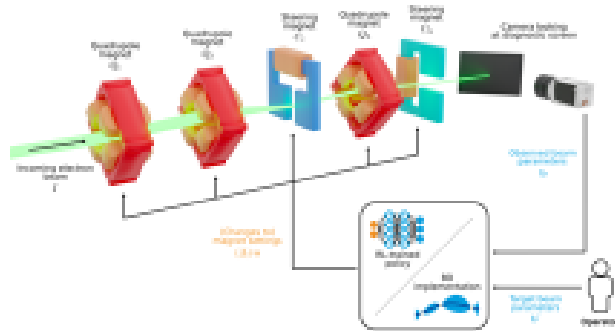
A. Santamaria Garcia, C. Xu, L. Scomparin, E. Bründermann,
M. Caselle, G. De Carne, A. -S. Müller



First detailed comparison of BO and RL in a real accelerator

J. Kaiser, C. Xu et al. arXiv: 2308.03739

- **Task:** focus and position the electron beam
- **Actuators:** 3 quadrupole magnets + 2 corrector magnets
- **Observation:** beam image on the diagnostic screen



RL optimization outperforms BO

Damping of transverse oscillations in KARA

First RL algorithm online training and running on hardware in accelerators

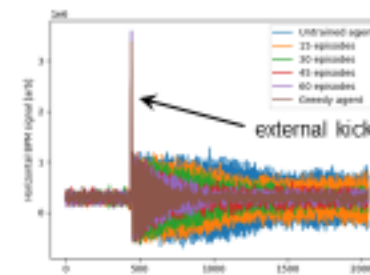


Reinforcement Learning

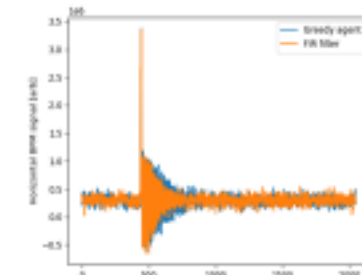
- **Agent:** Vanilla PPO from Stable Baselines 3
- **Actor & critic architecture:** 8-16-1
- **Reward:** metric of the beam position (low as possible)
- **Observation:** last 8 BPM samples
- **Strategy:**
 1. Agent acts during 2048 turns (0.74 ms)
 2. Agent stops and is re-trained in a CPU (~2.8 s)
 3. New weights are sent to Versal board and agent starts again



- NNs coded in Versal AIE
- Only forward pass



Damping improves with experience: the system is learning!



Achieves (sometimes surpassing) performance of FIR filter control (commercial solution)

L. Scoparin

DFCSR: A Fast Calculation of 2D/3D Coherent Synchrotron Radiation in Relativistic Beams

Jingyi Tang on behalf of:
Gennady Stupakov and Zhirong Huang

8/31, 2023



U.S. DEPARTMENT OF
ENERGY

Stanford
University

SLAC NATIONAL
ACCELERATOR
LABORATORY

DFCSR, can simulate 2D/3D CSR and space charge wakes in relativistic electron beams 2 or 3 orders of magnitude faster than conventional models like CSRtrack with 2 or 3 orders of magnitude more particles for better resolution.

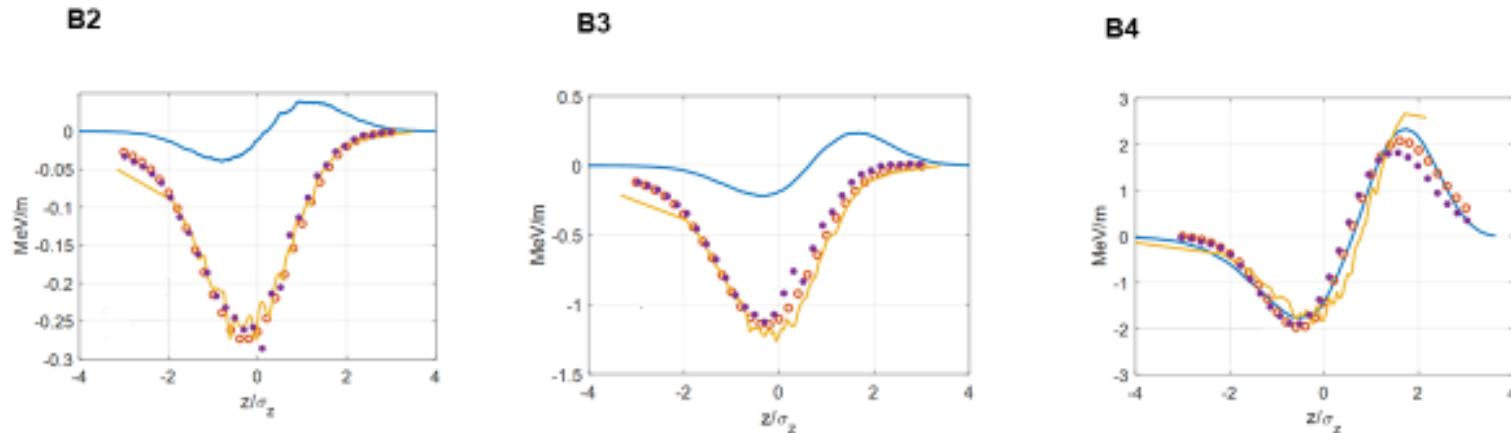
- Open Source
- Bench marked wth dipole, FACET II Chicane, Berlin Benchmark Chicane

Berlin Benchmark Chicane

SLAC



- 1D ELEGANT
- DFCSR Gaussian
- CSRtrack
- DFCSR Tracking



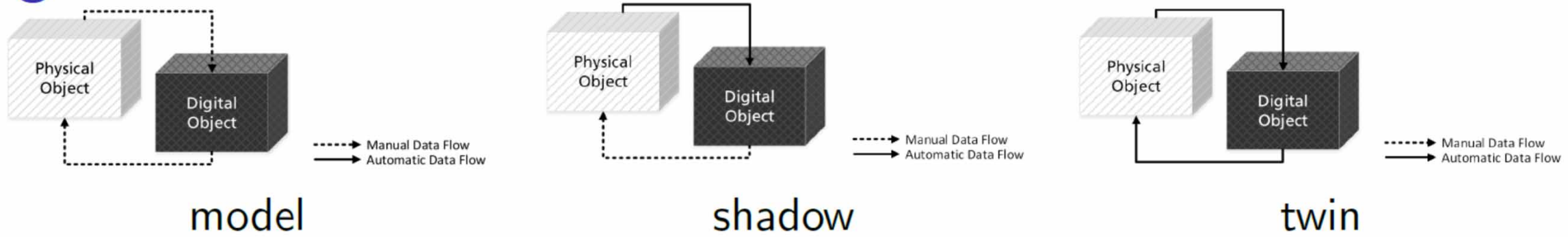
Building Digital Models with thor_scsi An Evolutionary Approach

Waheedullah Sulaiman Khail, Pierre Schnizer, Paul Goslawski

Helmholtz-Zentrum Berlin (HZB), Germany

Tracy is used as a computing core for digital models for synchrotron light sources since SLS. It inspired the accelerator toolbox, which is using (largely) Tracy's Hamiltonian propagators. This **Tracy** code was refactored using modern software paradigms and renamed to **thor-scsi**. Digital shadows or twins are essential ingredients for building 4th generation light sources. Based on the modernized thor_scsi code we built an EPICS IOC exporting required thor_scsi externals as EPICS variables. While it focuses on HZB's current BESSY II and MLS, it is designed flexibly to extend to the BESSY III and MLS II project or similar light sources.

Digital twin: nomenclature



Marek Grabski (MAXIV) ID: 2661 - TH4D1
Overview and Challenges of the Vacuum
Systems of Diffraction Limited Storage Rings

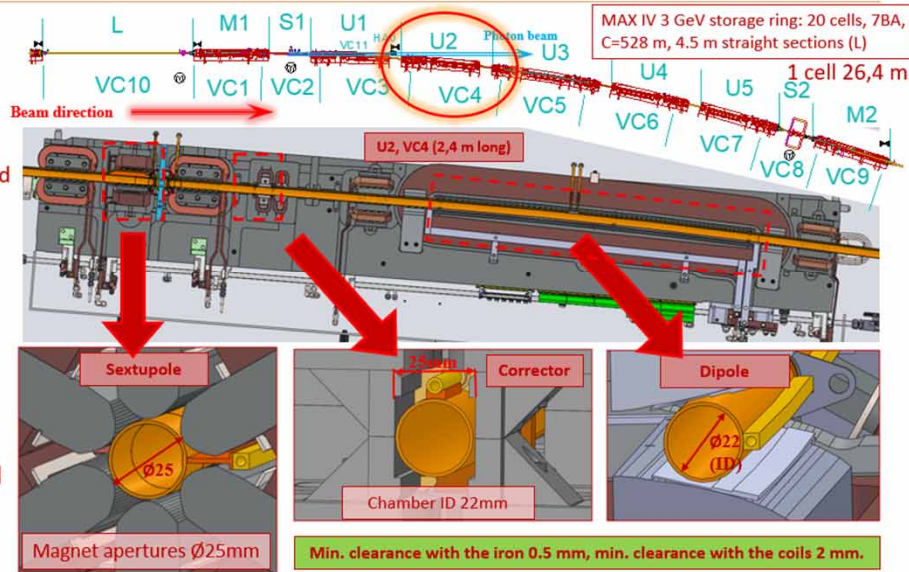
Design approach 1: NEG coating, distributed absorbers

NEG coated copper tubes, with distributed absorbers at MAXIV (similar at Sirius).

At MAX IV magnets are embedded in a closed magnet block.

Limited lumped pumping in standard cell:

- MAX IV - 3 pumping ports with ion pumps (75 l/s), 1 crotch absorber,
- Sirius - 5 pumping ports with ion pumps (20 l/s) and NEG cartridges (200 l/s), 3 crotch absorbers,

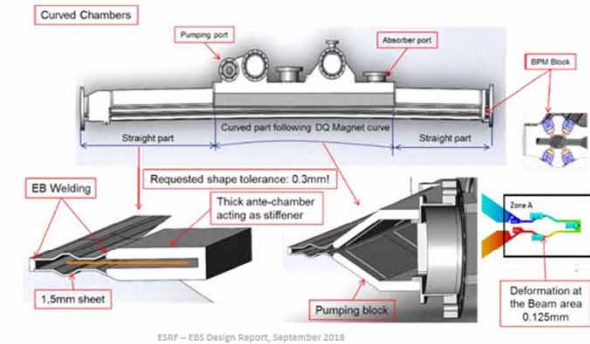


Design approach 2: Lumped absorbers and pumps

Conventional: Stainless steel and aluminium vacuum chambers with antechambers, lumped vacuum pumps and photon absorbers, NEG coating only in ID chambers (ESRF-EBS)



Stainless steel Vacuum chambers: 316 LN, 316 L



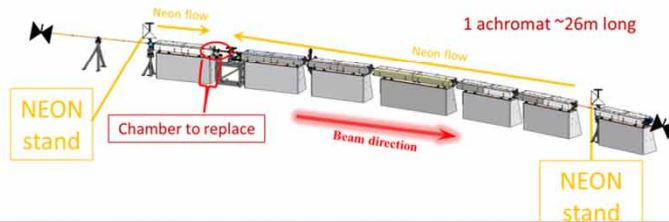
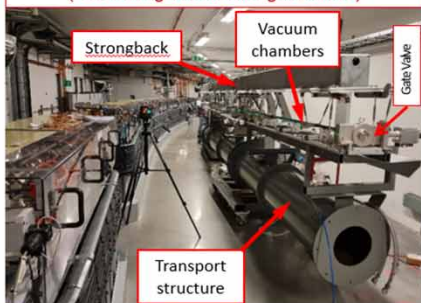
Design aspect: Serviceability

The more compact the lattice the more difficult is to do maintenance/exchange vacuum system components (limited access)

Options for service/exchange:

- Have one complete cell of vacuum chambers (spare achromat) assembled under vacuum with NEG activated (need to open all magnets),
- Make use of in-situ baking system if available to bake/activate NEG (no need to open all the magnets),
- If no in-situ baking system available need to bake/activate NEG outside the magnets with an oven (need to open all magnets),
- Use of Neon venting (to avoid need of NEG reactivation and no need to open all the magnets) (confirmed at MAXIV, Sirius, CERN),

MAX IV: One spare vacuum cell inside accelerator tunnel on a transport structure (~22 m long without straight section)

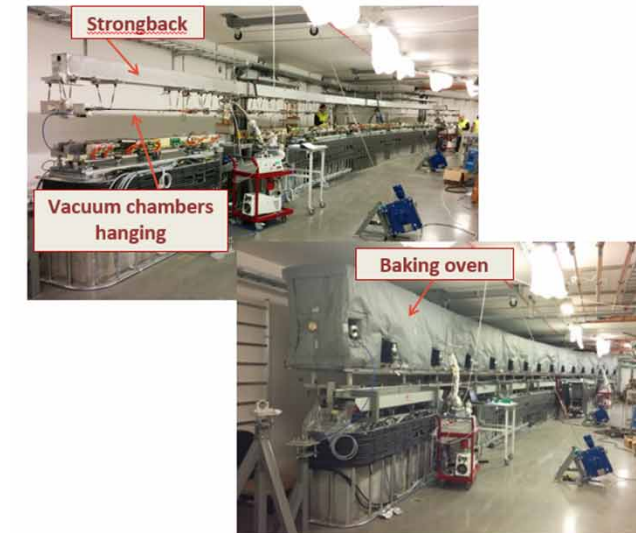


Neon venting is a procedure developed and used at CERN for interventions on special vacuum chambers with NEG coating. Neon is a noble gas, it does not saturate the NEG surface. Therefore there is no need of re-activation of the NEG film.

At MAX IV Neon venting used in 2018 and 2020 for interventions. No limitation in storage ring performance was observed after ~10 A h beam dose.

Design aspect: Installation (baking: Ex-Situ, in-situ)

Ex-situ installation and baking with an oven (MAX IV).

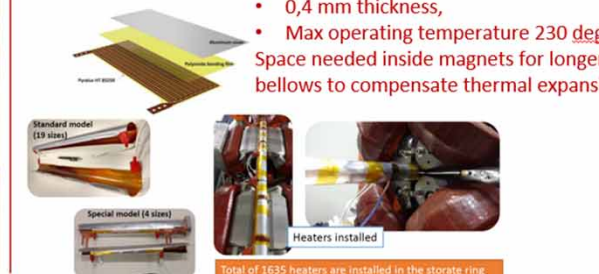


Installation and In-situ baking with thin heater system (Sirius, ESRF-EBS).



Thin heater system at Sirius:

- 0,4 mm thickness,
 - Max operating temperature 230 deg C.
- Space needed inside magnets for longer bellows to compensate thermal expansion



DLS summary

Chosen Diffraction Limited Storage rings in operation, installation and design:

Facility	New/ Retrofitted; commissioning year	Circumference [m]; (# of cells - Lattice)	Energy [GeV]; current [A]; emittance [pm.rad]	Magnet bore [mm]; chamber aperture [mm]	Vacuum system design approach	Vacuum chamber material	% of chambers NEG coated (lengthwise)	# of lumped pumps per cell	Baking/ activation method
ALS-U, USA	Retro; 2026	196; (12 cell - 9BA)	2; 0,5; 70	24; 13-20	Hybrid*	St. steel, copper,	60	3-4	In-situ
APS-U, USA	Retro; 2024	1104; (40 cell - 7BA)	6; 0,2; 60	26; 22	Hybrid*	St. steel, copper, Aluminum	40	9+4 NEG strips	In-situ
Diamond II, UK	Retro; 2027	560; (24 cell - MH6BA)	3,5; 0,3; 161	24; 20	Hybrid*	St. steel, copper, Aluminum	>90	8	Ex-situ
ESRF EBS, France	Retro; 2020	843; (32 cell - H7BA)	6; 0,2; 133	~28; 13-20	Conventional (lumped pumps and absorbers)	St. steel, Aluminum,	(only ID chambers in straights)	24	In-situ
HEPS, China	New; 2024	1360; (48 cell - H7BA)	6; 0,2; 34	24; 22	Hybrid*	St. steel, CrCrZr, and Inconel	70	14	In-situ
MAX IV, Sweden	New; 2016	528; (20 cell - 7BA)	3; 0,5; 300	25; 22	Distributed absorbers, NEG coating	Copper, (St. steel for ports and flanges)	>95 (fully)	3	Ex-situ
SLS 2.0, Switzerland	Retro; 2024	288; (12 cell - 7BA)	2.7; 0,4; 159	22; 18	Distributed absorbers, NEG coating	Copper, (St. steel for BPMs)	>95 (fully)	14	Ex-situ
Soleil II, France	Retro; 2028	354; (20 cell - 12 x 7BA + 8 x 4BA)	2,75; 0,5; 80	16; 12	Distributed absorbers, NEG coating	CuCrZr (full chambers), copper	>95 (fully)	4 / 7 (1 per dipole)	Ex-situ

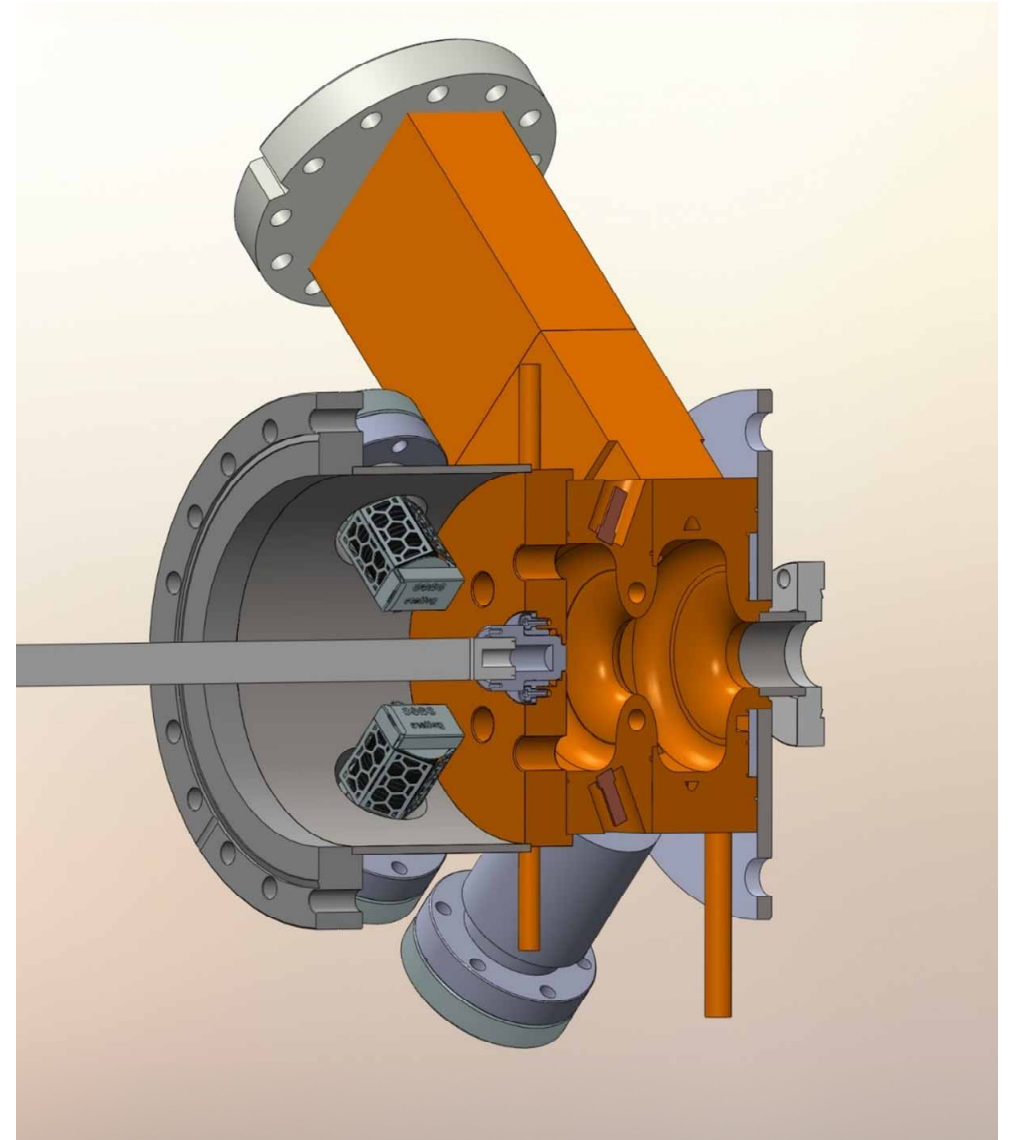
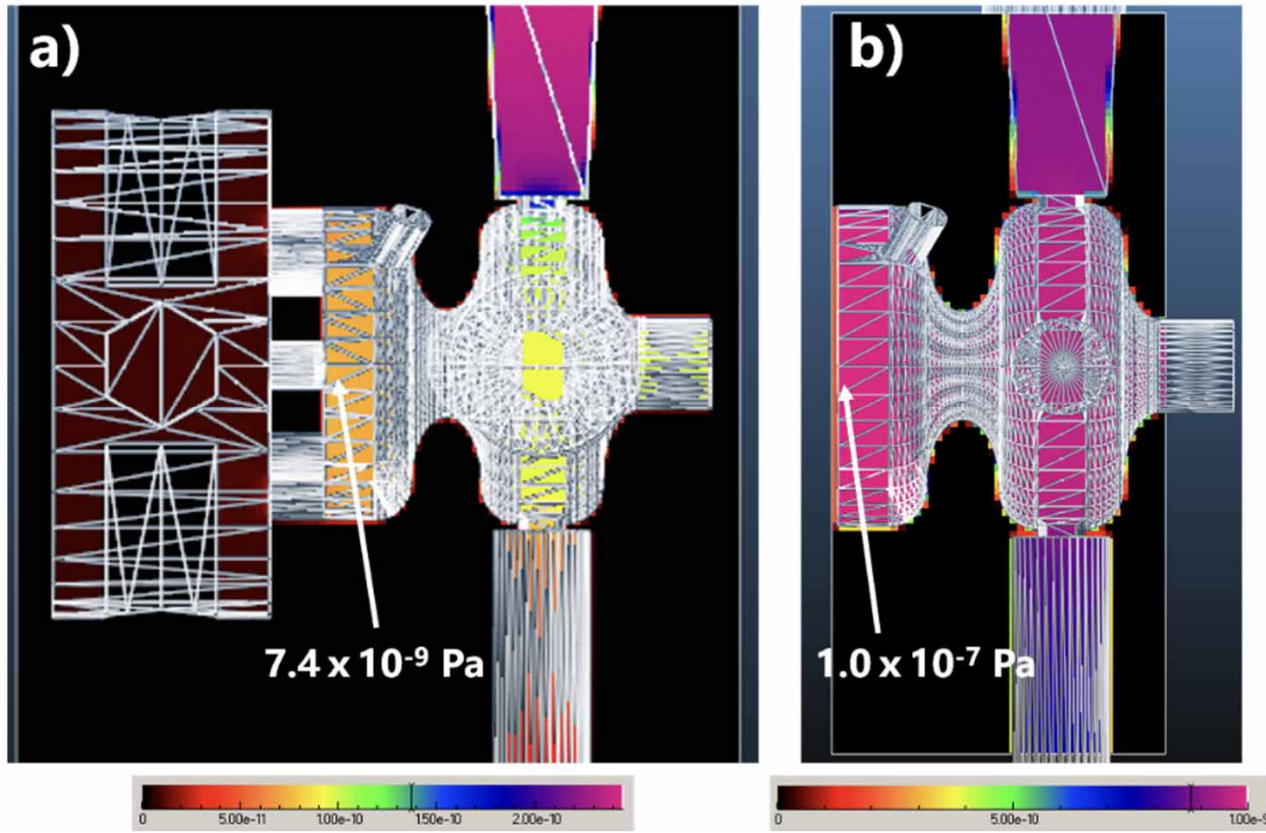
Not in the table: Sirius, Alba II, Elettra 2.0, Petra IV, BESSY III, Spring-8 II, HALF, SPS II.

* Hybrid: Distributed absorbers and NEG coating, also lumped pumping and lumped absorbers.

Renkai Li (TUB) ID: 2621 - TH4D2 An Ultra-
high Vacuum, High-gradient RF Gun and
Advanced Photocathode Studies

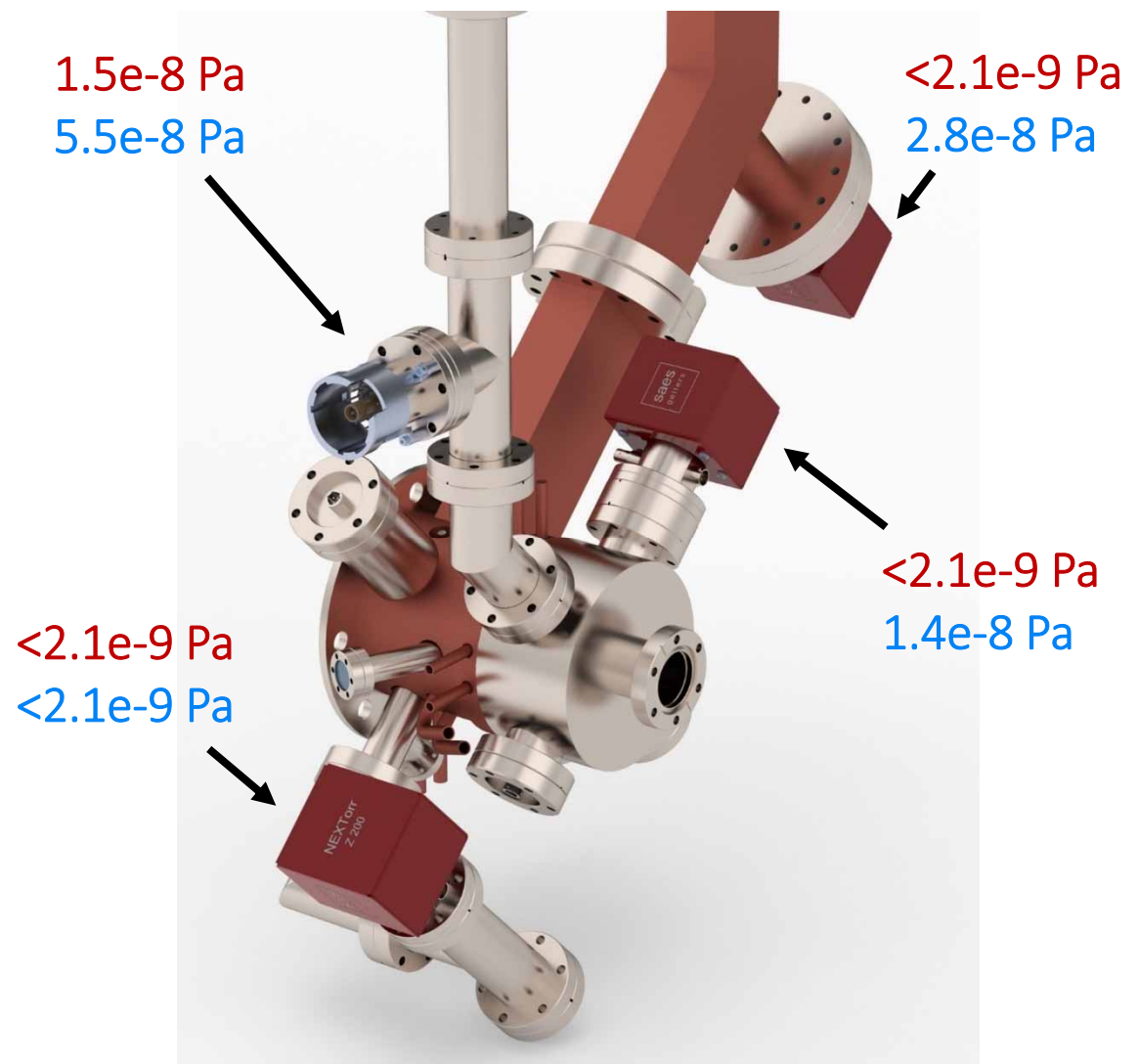


>10 fold improvement in vacuum at cathode surface

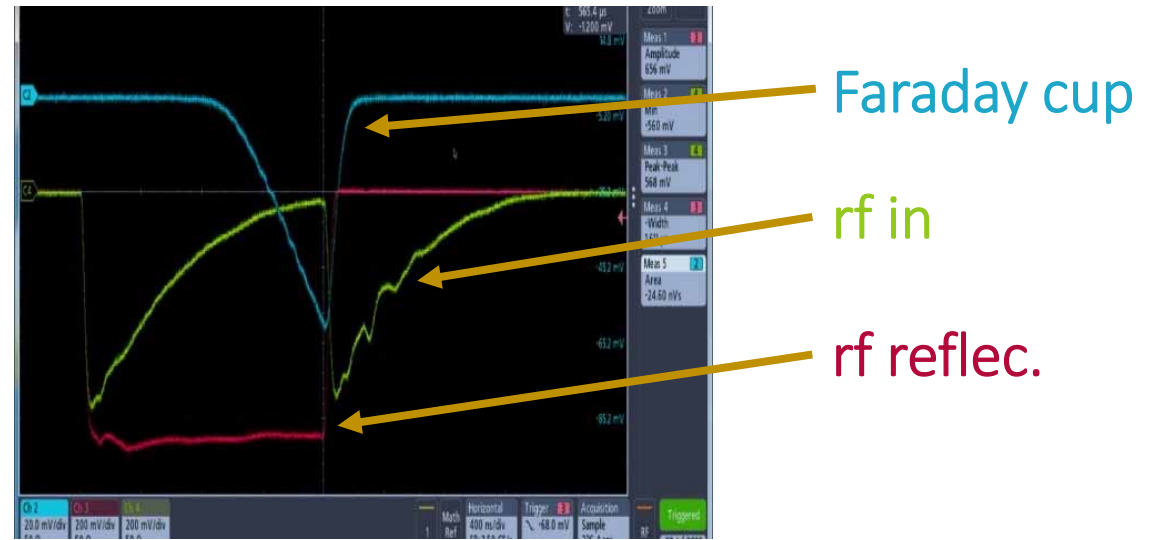


P. W. Huang et al., NIMA 1051, 168251 (2023)

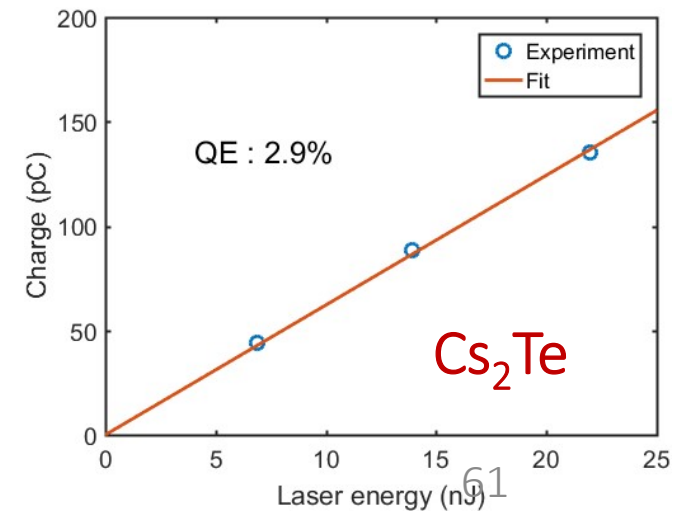
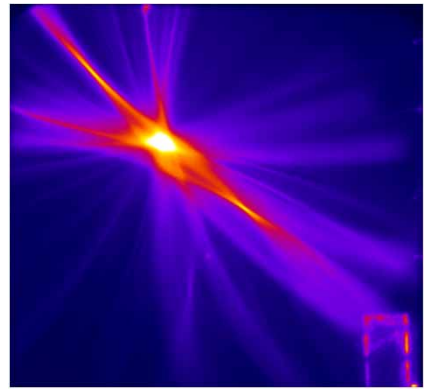
Base/operation pressure



rf conditioning after 24 hrs



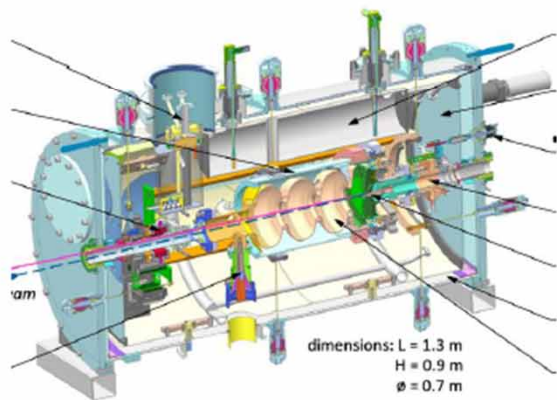
Dark current 0.5 nC @
 $E_z \sim 105$ MV/m



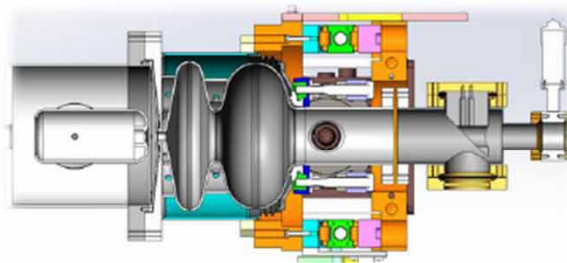
Rong Xiang (HZDR) ID: 2481 - TH4D3 Status
of Advanced Photocathodes for SRF Guns

1. Introduction

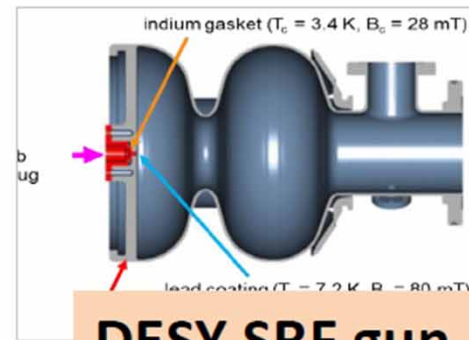
SRF guns for CW high brightness beam



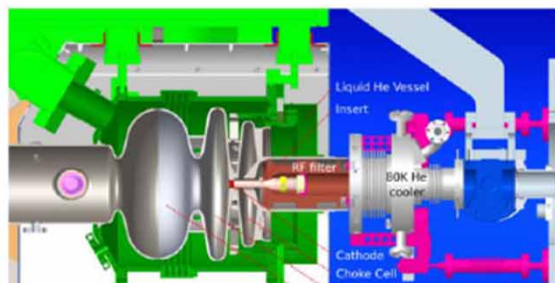
**HZDR SRF gun-II
in user operation**



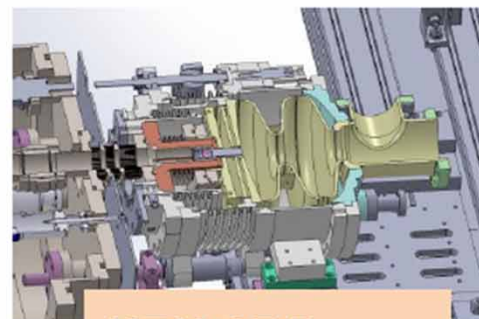
PKU DC-SRF gun



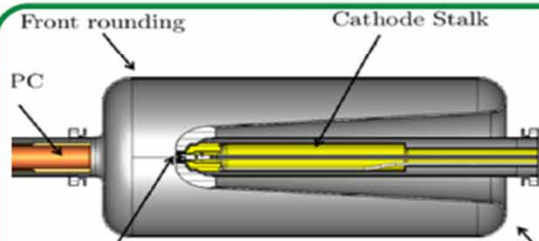
DESY SRF gun



HZB SRF gun

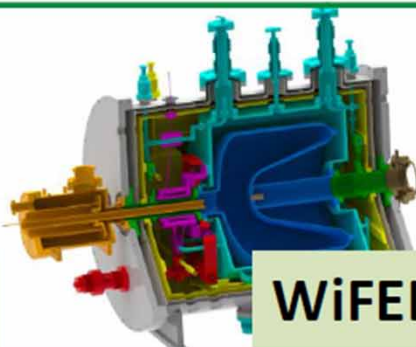


KEK SRF gun

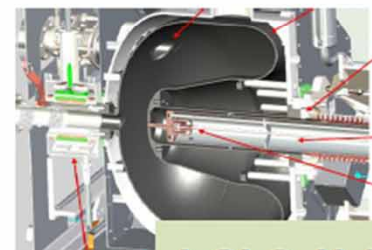


emp 300 K

BNL SRF gun



WIFEL gun



LCLS-II HE gun

2. Normal conducting photocathodes for SRF guns

2.1 Metal photocathodes in SRF Guns

Metal	QE	ϕ (eV)	Tc (K)
Cu	$10^{-5} - 10^{-4}$	4.6	
Mg	$10^{-5} - 10^{-3}$	3.6	
Nb	$10^{-6} - 10^{-4}$	4.3	9.3
Pb	$10^{-6} - 10^{-3}$	4.2	7.2

9

2. Normal conducting photocathodes for SRF guns

2.2 Semiconductor photocathodes in SRF Guns

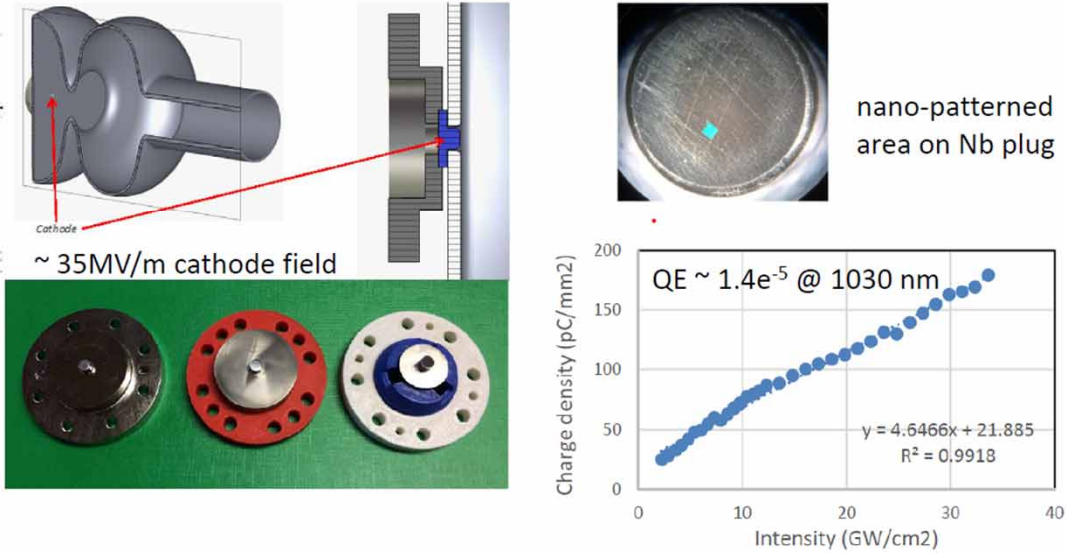
Cathode	Typical wavelength (nm)	QE @ room Temp.	$E_G + E_A$ (eV)	Expected thermal emittance ($\mu\text{m}/\text{mm}$)
Cs₂Te	266	0.1	3.5	0.9
Cs ₃ Sb	432	0.15	1.6+0.45	0.7
K ₃ Sb	400	0.07	1.1+1.6	0.5
Na ₃ Sb	330	0.02	1.1+2.44	0.4
Na₂KSb	330	0.1	1+1	1.1
K₂CsSb	532	0.1	1+1.1	0.4
GaAs(Cs,O)	532	0.1	1.4±0.1	0.44
GaN(Cs)	250-360	0.2-0.3	3.4 -?	-

D.H. Dowell et al., NIMA 622, Pages 685-697 (2010)

Xiaohui Wang et al., J. Mater. Chem. C, 2021, 9, 13013

3. Superconducting photocathodes for SRF guns

SC photocathode: Plasmonic Nb cathode @ Jlab / RadiaBeam



F.E. Hannon, et al., IPAC2019, TUPTS069, Melbourne, Australia

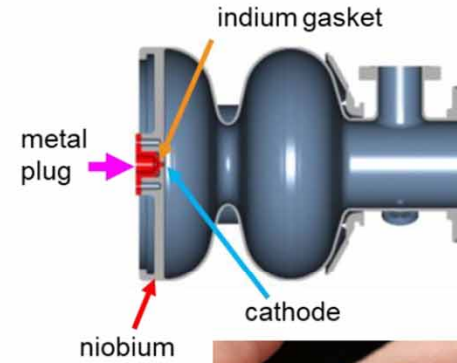
3. Superconducting photocathodes for SRF guns

SC photocathode for DESY SRF gun

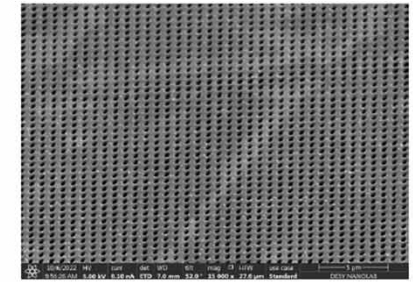


Status: *in developing*

1. Pb coating on Nb plug (or Cu Plug)
 - QE reached 2.7×10^{-3} @ 213 nm
 - air-stable photocathode
 - better adhesion required
2. Surface plasmon enhanced Nb (or Cu)



courtesy of D. Bazyl, E. Vogel



Nanostructured Cu (credit: DESY NanoLab)

16 E. Vogel et al., SRF2019,THP080; J. Lorkiewicz et al., Vacuum, Volume 179, Sep. 2020, 109524

Key Technologies Working Group D

- 19 presentations across 5 sessions
- Thanks to all the speakers for your excellent, high quality, presentations and uploading them all promptly !
- Thanks to my co-convenors for helping me put this summary together